Zeitschrift: Schweizerische mineralogische und petrographische Mitteilungen = Bulletin suisse de minéralogie et pétrographie

Band: 75 (1995)

Heft: 2

Vereinsnachrichten: Bericht über die 69. Hauptversammlung der Schweizerischen Mineralogischen und Petrographischen Gesellschaft in Aarau = 69. annual meeting of the Swiss Society of Mineralogy and Petrogrology at Aarau

SCHWEIZ. MINERAL. PETROGR. MITT. 75, 291–322, 1995

Bericht über die 69. Hauptversammlung der Schweizerischen Mineralogischen und Petrographischen Gesellschaft in Aarau

6. Oktober 1994

69. annual meeting of the Swiss Society of Mineralogy and Petrology at Aarau

October 6, 1994

Zusammenfassungen der Vorträge und Posters

Abstracts of communications and posters

Th. Adatte and G. Keller (Neuchâtel, Princeton):

Clay-mineral correlation across the Paleocene-Eocene boundary: evidence for global turnover from Western to Eastern Tethys?

Faunal and carbon isotopic data from Caravaca and Zumaya (Spain) indicate that the Paleocene-Eocene (PE) event in the western Tethys which affected the entire water column leading to the sudden extinction of 50% of benthic foraminifera and the more gradual extinction of 33% of planktic foraminifera, corresponds to an abrupt change in whole rock and clay mineral composition.

The Paleocene-Eocene transition at Zumaya (northern Spain) consists of 20 m of homogenous grey marls intercalated with calcarenite layers (biozones P4 to upper P6a) and 20 m of marls alternating with grey limestone beds (upper Zone P6a and P6b). A dark grey shale layer marked by carbonate dissolution and the main benthic extinction event characterizes the onset of the $\delta^{13}C$ short term negative shift. At Caravaca (southern Spain), sediments consists of 40 m of grey marls intercalated with thin grey limestone beds (Zone P4) and two laminated dark grey shale layers marked by carbonate dissolution and condensation that characterized the $\delta^{13}C$ shift and subsequent low $\delta^{13}C$ values. A small hiatus is detected in a limestone layer 2.5 m below the $\delta^{13}C$ shift, where the zone P5 and the lower part of P6a are missing.

Whole rock components are identical in the two sections with calcite, quartz, plagioclase, K feldspars. An abrupt change is observed in both sections marked by an increase in quartz (up to 50%), phyllosilicates and feldspars, coinciding with calcite decrease. This increase in detrital influx takes place in the upper zone P6a in both sections, just below the $\delta^{13}C$ negative excursion and reflects significant paleo-environmental change. Clay minerals recognized at Zumaya consist of smectite, mica, mixed-layers, kaolinite and chlorite. Kaolinite appears 6 m below the PE boundary, corresponding to significant decrease in smectite and chlorite. Kaolinite, chlorite, smectite and mica are present at Caravaca, as well as palygorskite and sepiolite. Similar to Zumaya, significant amounts of kaolinite are present 2 m below the PE transition coinciding with a decrease in sepiolite, palygorskite and smectite.

In both sections, kaolinite occurrence is restricted to the P6a-lower P6b interval and therefore correlates exactly with the short term $\delta^{13}C$ negative excursion. Palygorskite and sepiolite generally indicate warm and arid climates associated with enhanced evaporation. In contrast, kaolinite typically develops in tropical soils on

well drained surface which receive high precipitation. Moreover palygorskite and sepiolite are commonly found in the adjacent continental areas where kaolinite is not present, indicating arid environments. These data suggest that only a global turnover of oceanic circulation (change in source area of bottom water) can explain the massive extinction of the benthic community and the presence of kaolinite close to coastal areas in low and middle latitudes, where arid conditions prevailed during the Paleocene-Eocene transition.

M. Berger (Bern):

The charnoenderbites of the Northern Marginal Zone of the Limpopo Belt, Zimbabwe: a test of Archean crust formation models (see also Schweiz. Mineral. Petrogr. Mitt. 75/1, 17–42).

The Limpopo Mobile Belt, situated between the Zimbabwe and Kaapvaal Cratons in Southern Africa, is a tectonic province with a complex history stretching in time from over 3.0 Ga to around 2.0 Ga. According to different structural trends and lithologies the belt has been subdivided into three zones (COX et al., 1965; MASON, 1973): the Northern Marginal Zone (NMZ), the Central Zone (CZ) and the Southern Marginal Zone (SMZ). The Northern Marginal Zone in Zimbabwe is separated from the Central Zone by the dextral Triangle Shear zone and is juxtaposed to the amphibolite facies tonalites of the Zimbabwe Craton in the north by a major thrust, which operated around 2.6 Ga (MKWELI et al., 1994). The NMZ is dominated by granulite facies, tonalitic to granodioritic rocks refered to as the charnoenderbitic suite. These rocks carry a more or less strongly developed ENE–WSW trending gneissic fabric. Mainly basing on the structure of the belt tectonic models involving Archean continent-continent collision (ROERING et al., 1992; TRELOAR et al., 1992) or terrane accretion (ROLLINSON, 1993) have been proposed as a reason for the crustal thickening observed. Since KAMBER et al. (1994) showed that the movement along the Triangle Shear zone took place at around 2.0 Ga, the main argument for Archean continent-continent collision is discounted (see HOLZER et al., p. 302 this volume) and the factual reason for Archean crustal overthickening must be determined. Main subject of my studies is the petrogenesis of the charnoenderbitic suite of the NMZ which represents Archean middle to lower crust (paleodepth ~ 20–25 km).

Field and petrological data suggest that the charnoenderbite suite rocks crystallized as granulites directly from a melt, rather than being metamorphosed to granulite grade. Petrological evidence for a magmatic suite comprises the igneous textures of these rocks and the non-existence of prograde replacement textures in the charnoenderbites. On the other hand, symplectitic replacement textures of clino- and orthopyroxene, quartz and magnetite consuming amphibole are developed in mafic xenoliths and larger remnants of mafic supracrustal material which are incorporated in the charnoenderbites.

Well defined trends of major and trace elements indicate fractionation of clinopyroxene, plagioclase, + biotite and possibly orthopyroxene to be the mechanism of differentiation of the rocks examined. In addition it was found that the NMZ has very similar geochemical characteristics to the Zimbabwe craton which is in contradiction with the terrane accretion model.

To constrain the timing of crustal growth, U–Pb zircon- and whole rock Nd model ages have been determined. Three samples of massive, homogeneous enderbite were analyzed for U–Pb and yielded upper intercept ages of 2603 ± 77 Ma, 2637 ± 19 Ma and 2710 ± 38 Ma. These ages are interpreted to represent the intrusion ages of the corresponding plutons. Sm–Nd isotopic composition was determined. The Nd T_{DM} ages of six enderbite whole rock samples, including the three which were also analyzed for U–Pb on zircon, lie in a narrow range between 2.96 and 3.08 Ga (calculated for the model of GOLDSTEIN et al., 1984). The model ages are in great contrast to the intrusion ages of 2.58–2.71 Ga. Even T_{CHUR} ages lie in a very narrow range and are in average 100 Ma older than the intrusion (U-Pb) ages of the charnoenderbites. The Nd model ages may either reflect a distinct crust forming event (= province age), or they may be interpreted as a subsequent extraction of melt from the depleted mantle coupled with the recycling of older crustal material.

The present data argue strongly against tectonic models such as a subduction related island arc setting or terrane accretion as a reason for Archean crustal overthickening and a granulite facies metamorphism in the NMZ, but they do support a model involving continuous magmatic crustal growth under dry conditions leading to an anomalously thick portion of crust, generated in a time span between 2.6 and 2.75 Ga.

COX, K.G., JOHNSON, R.L., MONKMAN, L.J., STILLMAN, C.J., VAIL, J.R. and WOOD, D.N. (1965): The geology of the Nuanetsi igneous province. Phil. Trans. R. Soc. London, A 257, 71–218.

GOLDSTEIN, S.L., O'NIONS, R.K. and HAMILTON, P.J. (1984): A Sm–Nd isotopic study of atmospheric dusts and particulates from major river systems. Earth and Planet. Sci. Lett., 70, 221–236.

KAMBER, B.S., KRAMERS, J.D., NAPIER, R., CLIFF, R.A. and ROLLINSON, H.R. (1994): The Triangle Shear-zone, Zimbabwe, revisted: New data document an important event at 2.0 Ga in the Limpopo Belt. Prec. Res., in press.

MASON, R. (1973): The Limpopo Mobile Belt – Southern Africa. Phil. Trans. R. Soc. London, A 273: 463–485.

ROERING, C., VAN REENEN D.D., SMIT, C.A., BARTON, J.M.J., DE BEER, J.H., DE WIT, M.J., STETDER, E.H., VAN SCHALKWYK, J.F., STEVENS, G. and PRETORIOUS, S. (1992): Tectonic model for the evolution of the Limpopo Belt. Prec. Res., 55, 539–552.

ROLLINSON, H.R. (1993): A terrane interpretation of the Archean Limpopo Belt. Geol. Mag., 130, 755–765.

TRELOAR, P.J., COWARD, M.P. and HARRIS, N.B.W. (1992): Himalayan-Tibetan analogies for the evolution of the Zimbabwe Craton and Limpopo Belt. Prec. Res., 55, 571–587.

MKWELI, S, KAMBER, B. and BERGER, M. (1994): Westward Continuation of the Craton-Limpopo Belt tectonic Break in Zimbabwe and new age constraints on the timing of the thrusting. J. geol. Soc., in press.

Peter Berlepsch (Basel):

Kristallstrukturelle und -chemische Untersuchungen an Edenharterit ($TlPbAs_3S_6$) (siehe p. 277–281 in diesem Heft).

Crystal structure and chemical composition of Edenharterit ($TlPbAs_3S_6$) (see p. 277–281 in this issue).

Giuseppe G. Biino, Thomas C. Meisel, Thomas F. Nägler and Jan D. Kramers (Fribourg, Bern):

Whole rock chemistry and isotope chemistry of metasediments in the Silvretta nappe and the early crustal history of the Alpine basement.

The geological history of the Alps is characterized by several large events which took place over a long time-span covering at least the last 600 Ma and involving crustal material of, in part, at least 1.7 Ga age. An old basement, having already experienced a pre-Variscan orogenic phase, has been clearly identified in several Alpine tectonic units (Helvetic, Silvretta, Tauern Window, Berisal, and Strona Ceneri basements). The Late Ordovician post orogenic granitic magmatism is the best marker to distinguish this old basement (MERCOLLI et al., 1994). It is made up of metasediments and mafic-ultramafic rocks. The absolute age for the deposition of the older sediments is poorly constrained, but it should be Late Proterozoic or Early Palaeozoic (for a review see GEBAUER, 1993; SCHALTEGGER, 1994).

Investigations on the Silvretta nappe, summarized by MAGGETTI and FLISCH (1993), have shown a complex geological history involving an ocean floor environment, subduction and collision. In this study we address the metasediments of the Silvretta basement and use whole rock geochemistry plus Sr, Pb, and Nd isotopes to test and constrain pre-Variscan tectonic models.

According to major element discriminatory treatment (ROSER and KORSCH, 1988) the metasediments should be related to an active continental magmatic arc with important detritus from a mature continental source. Mafic and ultramafic contribution to the sediments is doubtful. Trace element data (Th, Sc, La, Co, Zr plots after BHATIA and CROOK, 1986) point to provenance from a dissected magmatic arc and recycled orogen: the nature of the eroded crust should be an island arc with significant continental input. As several studies have shown that geochemical datasets from contrasting tectonic environments overlap significantly, and geochemical discrimination should be done with caution, isotopic work should complement this type of study. If the sedimentary protoliths were generated from sources having distinct isotopic signatures, isotopic investigation may detect differences in initial isotopic ratio and help to identify and characterize parental material and geodynamic setting. Micaschists show higher $^{87}Sr/^{86}Sr$ ratios (at present time ranging between 0.735–0.740) than paragneisses ($^{87}Sr/^{86}Sr$ ~ 0.720). However, between 600 Ma and 500 Ma, initial $^{87}Sr/^{86}Sr$ compositions approach each other. Therefore, the suggestion of GRAUERT (1969), i.e. an imprinting of the dominant isotopic signature around 600–500 Ma, is supported. Micaschist shows a more negative $\varepsilon Nd_{(0)}$ than the paragneiss, and micaschist defines a model age of approximately 1.9 Ga (but paragneiss of 1.7 Ga). These ages are clearly unrelated to deposition age. 1.7 Ga is typical for much of the rock of central Europe, but 1.9 Ga is rather rare. It suggests that tectonic events (even if important mass exchange occurred) did not modify the Nd–Sm isotopic system, or more probably that a large volume of the present European crust has not seen addition of juvenile crust for a long time and it is a well homogenized reservoir. Common lead suggests a derivation from a Late Proterozoic or Lower Palaeozoic upper crust, but differences exist between micaschist and paragneiss. Micaschist shows higher $^{207}Pb/^{204}Pb$ and lower $^{206}Pb/^{204}Pb$ than paragneiss (the range in $^{208}Pb/^{204}Pb$ ratio is comparable), showing that it was derived from an older source (with high U/Pb) than the latter. Thus Pb, Nd, and Sr data are in agreement.

In a few outcrops, micaschist has been metasomatized by fluid infiltration during postoro-

genic (Variscan) extension. Metasomatism is also responsible for P1 replacement mainly of Ms (knotengneiss formation). The Rb–Sr isotopic system has been perturbed (present day $^{87}Sr/^{86}Sr$ ratios range from 0.735 to 0.730) suggesting that the fluid was in equilibrium with rocks characterized by lower $^{87}Sr/^{86}Sr$ ratios relative to normal micaschist (an isotopic composition comparable to that of the paragneiss or metagranite). The same samples show increased $^{207}Pb/^{204}Pb$, $^{206}Pb/^{204}Pb$, and $^{208}Pb/^{204}Pb$ ratios relative to normal micaschist.

Since the main concern in this work is with the Late Proterozoic and early Palaeozoic history, we can make only very general assumptions concerning tectonic settings due to the few independent constraints. Nevertheless, our data appear to be in agreement with the model of accretion along a pre-Caledonian active margin.

BHATIA, M.R. and CROOK, K.A.W. (1986): Trace element characteristics of graywackes and tectonic setting discrimination of sedimentary basins. Contrib. Mineral. Petrol. 92, 181–193.

GEBAUER, D. (1993): The pre-Alpine evolution of the continental crust of the central Alps – an overview. In J.F. VON RAUMER and F. NEUBAUER (eds): Pre-Mesozoic geology in the Alps. Springer-Verlag, 93–117.

GRAUERT, B. (1969): Die Entwicklungsgeschichte des Kristallins auf Grund radiometrischer Altersbestimmungen. Unpubl. Ph. D. Thesis, Universität Bern, 166 pp.

MAGGETTI, M. and FLISCH, M. (1993): Evolution of the Silvretta Nappe. In J.F. VON RAUMER and F. NEUBAUER (eds): Pre-Mesozoic geology in the Alps. Springer-Verlag, 469–482.

MERCOLLI, I., BIINO, G.G. and ABRECHT, J. (1994): The lithostratigraphy of the pre-Mesozoic basement of the Gotthard massif. Schweiz. Mineral. Petrogr. Mitt. 74, 29–40.

ROSER, B.P. and KORSCH, R.J. (1988): Provenance signatures of sandstone-mudstone suites determined using discriminant function analysis of major-element data. Chem. Geol. 67, 119–139.

SCHALTEGGER, U. (1994): Unravelling the pre-Mesozoic history of Aar and Gotthard massifs (Central Alps) by isotopic dating – a review. Schweiz. Mineral. Petrogr. Mitt. 74, 41–51.

Giuseppe G. Biino and Claire Prospert
(Fribourg):

Petrology of polymetamorphic metasediments: an example from the Silvretta nappe.

The basement of the Silvretta nappe is composed of metasedimentary rocks, metagranites and mafic (very minor ultramafic) rocks. Mafic rocks exhibit polymetamorphic evolution (MAGGETTI and FLISCH, 1993, with references therein). Metasedimentary rocks mainly show textures and minerals developed during the (Late ?) Variscan amphibolite facies metamorphism (petrogenetic grids for the metasedimentary rocks will be presented at the meeting). Evidence for polymetamorphic evolution of the sedimentary rocks is very slight, but it is reasonable to consider that mafic and sedimentary rocks underwent the same metamorphic evolution. The amphibolite facies reequilibration shows a general increase in metamorphic gradient from SE toward NW. It is interesting to note that the same orientation of the amphibolite metamorphic facies gradient has been observed in the Helvetic basement of the central Alps. With the present state of the art, it is difficult to decide how many pre-Alpine metamorphic cycles occurred in the Silvretta nappe. Two dominant models may be proposed. According to a monocycle model, all the pre-Alpine metamorphic evolution occurred during Variscan (both eclogite and amphibolite facies overprints). In this case, the Ordovician granitoids also underwent HP metamorphism. Alternatively, HP metamorphism is part of an older cycle (Caledonian?), and the amphibolite facies metamorphism is related to Variscan events. Micaschist is often rich in staurolite. Staurolite shows two stages of growth. In the staurolite core, quartz inclusions evidence an old foliation completely overprinted in the rock matrix. In the staurolite rim, fibrolite and quartz inclusions are parallel to the main foliation of the rock. Indeed, chemical difference between core and rim has not been detected. It may indicate a decompression (according to Al_2SiO_5 polymorphs) path characterized by minor changes in temperature. A very peculiar rock type is made up of large (up to a few centimeters long) P1 porphyroclasts. This rock type was formerly a micaschist, but following P1 blastesis it shows gneissic texture (knotengneiss, KG). P1 includes Qtz + Grt + Bt + Ores and corroded Ms. Pl is deformed (PROSPERT and BIINO, see p. 314 this volume), but clearly superposes older microfolds. KG is frequently associated with Qtz + And veins. Several processes may be responsible for KG genesis. We therefore present families of solutions; choices between them must be based on their relative geological plausibility.

1) Ms breaks down to P1 during decompression after HP event. KG formation is related to the expansion of the stability field of Pl during decompression. This is the classical model already proposed by several authors. Uplift of a HP unit suggests a short time span (a few Ma) between HP metamorphism and extension (one orogenic cycle). Several arguments do not fully support this model. There is no microstructural evidence for an isochemical blastesis of Pl, and chemical transport is necessary to balance the

metasomatic reaction. In any case, fluids tend to escape a breakdown reaction site, and it is not easy to explain the observed metasomatism ($NaCaK_{-x}$). Feldspatized rocks only cover small areas, and the total amount of fluid produced by Ms break down is not enough to produce Pl blasts and Qtz-And veins. Chemical composition of the relic Ms is not consistent with HP Ms. Ms breakdown usually produces a different texture (e.g.: HEINRICH, 1982; ABRECHT and BIINO, 1994).

2) KG formed during a fluid infiltration episode coeval with Late Variscan extension. Neoblastic Pl have neither the shape of Ms (pseudomorph after Ms) nor can their grain sizes be reasonably to be due to a single metamorphic phase. Ms probably was the site of reaction (and one of the reacting phase) between the infiltrating fluid (Na–Ca rich) and the rock. Theoretical calculations on isobaric fluid-rock interactions show that during the cooling path of a hydrothermal fluid Qtz and K-bearing phase (Ms or K-fs) should precipitate and Pl dissolve. On the other hand, along the prograde fluid path Pl replaces a K-bearing phase (Ms or K-fs) and Qtz dissolves.

In the authors' view, the following model accommodates field and theoretical data. At the beginning of the extension, the Silvretta unit was mainly void of interstitial fluid. Due to tectonics, fluid started to infiltrate. Pl mostly formed before the main vein formation, when fluids moved along a prograde flow path. The same fluid should have also flowed along the retrograde trajectory to complete the flow path, and Qtz started to precipitate in veins. KG and Qtz + And veins formation are related, but they are not strictly contemporaneous at the same location.

Late Variscan metamorphism in the Silvretta nappe is characterized by extension. It is almost independent of the initial thermal conditions of the crust and could be mainly controlled by the extension rate and fluid infiltration. Any attempt to understand the thermal evolution of the Silvretta nappe must also take into account the influence of fluid flow on temperature distribution as fluid flow also involves heat transport.

ABRECHT, J. and BIINO, G.G. (1994): The metagabbros of the Kastelhorn area (Gotthard massif, Switzerland): Their metamorphic history inferred from mineralogy and texture. Schweiz. Mineral. Petrogr. Mitt. 74, 53–68.

HEINRICH, CH. (1982): Kyanite-eclogite to amphibolite facies evolution of hydrous mafic and pelitic rocks, Adula nappe, Central Alps. Contrib. Mineral. Petrol. 81, 30–38.

MAGGETTI, M. and FLISCH, M. (1993): Evolution of the Silvretta Nappe. In J.F. VON RAUMER and F. NEUBAUER (eds): Pre-Mesozoic geology in the Alps. Springer-Verlag, 469–482.

Ch. Böhm and M. Meier (Zürich):

Krustenentwicklung der Lucomagno-Kristallindecke (unteres Penninikum der Zentralalpen).

Crust evolution in the Lucomagno crystalline nappe (lower Penninic of Central Alps).

Während die traditionelle Gliederung der amphibolitfaziellen, polymetamorphen Gesteine der Lucomagno-Kristallindecke in 1) leukokrate Orthogneise und 2) glimmerreiche Paragneise bestätigt werden kann, verkörpern die 3) Augengneise entgegen früherer Autoren eindeutig metasedimentären Charakter. Folgende geochemische Kriterien erlauben diese Klassifikation:

– Hauptelementverteilungen für Ortho- resp. Paragneise liefern die Basis zur Unterscheidung von primär-magmatischen und sedimentären Metamorphiten nach SHAW (1972). Entsprechend dieser Klassifikation zeigen die Augengneise eindeutige Para-Zusammensetzungen. Im Feld bilden die Augengneise einzelne mit den vorherrschenden Paragneisen assoziierte Körper, entlang derer die Orthogneise in kleineren Linsen und Zügen auftreten.

– Tiefere Seltene Erden-Gehalte (S.E.tot = 112 ppm; 77–126 ppm) der Orthogneise stehen erhöhten Gehalten der Augengneise (S.E.tot = 169 ppm; 137–186 ppm) und Paragneise (S.E.tot = 175 ppm; 149–203 ppm) gegenüber. Starke Anreicherungen der leichten Seltenen Erden (La_N/Yb_N = 10; 7.1–15.8) und schwache bis ausgeprägte negative Eu-Anomalien (Eu/Eu* = 0.66; 0.50–0.90) in allen drei Hauptlithologien widerspiegeln relativ uniforme Seltene Erden-Verteilungen mit starker krustaler Komponente.

Erste leicht diskordante U/Pb-Analysen an altbestandsfreien Einzelzirkonen einer Orthogneisprobe ergeben ein vorläufiges Primäralter von ca. 288–296 Ma, woraus sich ein herzynisches Intrusionsalter der Orthogneise ableiten lässt. Damit kompatibel sind Rb/Sr-Gesamtgesteins-Isotopenanalysen an Orthogneisen, welche eine herzynische Errorchrone bilden. Variable initiale $^{87}Sr/^{86}Sr$-Verhältnisse (0.708–0.712 für 300 Ma) können neben Metamorphoseeinflüssen auf heterogene Magmenzusammensetzung sowie einen älteren Krustenanteil zurückgeführt werden. Die deutlich negativen initialen εNd-Werte der Orthogneise (–1.2 bis –6.0 für 300 Ma) bestätigen einen krustalen Anteil dieses Magmatismus.

Die herzynischen Orthogneise des Lucomagno lassen sich altersmässig direkt mit den spätherzynischen Intrusiva des Aar- und des Gotthardmassivs vergleichen (SCHALTEGGER, 1994; SERGEEV and STEIGER, 1994). Zusätzlich

zeigen die spätherzynischen Gneisstöcke des Gotthardmassivs (SERGEEV et al., 1993) analoge isotopengeochemische Signaturen zu den Orthogneisen des Lucomagno.

Die relativ hohen initialen $^{87}Sr/^{86}Sr$-Verhältnisse der Orthogneise weisen zusammen mit den ausgeprägt negativen initialen εNd-Werten sowie erhöhten Al-Sättigungsgraden (A/CNK = 1.0–1.32) auf peraluminöse S-Typ-Granite hin, welche mit der Verdickung kontinentaler Kruste in Zusammenhang stehen.

Nd-Mantelseparations-Modellalter der Orthogneise liegen zwischen 0.99 und 1.44 Ga und unterscheiden sich deutlich von älteren Modellaltern der Paragneise (TDM = 1.55–1.74 Ga) und Augengneise (TDM = 1.52–1.61 Ga), was die Anwesenheit einer jüngeren Mantelkomponente anzeigt.

SHAW, D.M. (1972): The Origin of the Apsley Gneiss, Ontario. Can. J. Earth Sci., 9, 18–35.
SCHALTEGGER, U. (1994): Unravelling the pre-Mesozoic history of Aar and Gotthard massifs (Central Alps) by isotopic dating – a review. Schweiz. Mineral. Petrogr. Mitt. 74, 41–51.
SERGEEV, S.A., MEIER, M. und STEIGER, R.H. (1993): Hercynian granitoid magmatism in the Gotthard massif: A discontinuous process? Abstr. SMPG-Tagung, Bagnes-Verbier, 107.
SERGEEV, S.A. und STEIGER, R.H. (1994): Time and Conditions of Continental Growth Processes in the Gotthard External Massif, Swiss Central Alps. Abstr. ICOG8, Berkeley, 285.

R. Bollin, G. Galetti, V. Liebetrau, M. Maggetti and U. Poller (Fribourg):

How useful are correlation diagrams for the discrimination ortho/para in metamorphic area? the case of the Silvretta.

In metamorphic areas it is difficult to macroscopically differentiate between orthogenic- and paragenic rocks, due to the strongly penetrating foliation. We have applied, on the Silvretta example, three geochemical discrimination-diagrams (Al_2O_3–MgO, THÉLIN, 1983; P_2O_5/TiO_2–MgO/CaO, WERNER, 1987; Zr/TiO_2–Ni, WINCHESTER and MAX, 1982). The biotite-bearing main lithologies of this Austroalpine crystalline unit were geochemically analyzed (over 500 analyses of meta-granites and -tonalites, ca. 200 analyses of the paragneisses). In the field, the transition from non-foliated to foliated granite is detectable and the acid, as well as the intermediate terms contain both, I- and S-type derivatives.

The evaluation shows, that the three diagrams, apart from a few exceptions, separate the series. The previous petrographic classification in ortho and para finds therefore also a geochemical confirmation.

THÉLIN, PH. (1983): Les gneiss œillés de la nappe du Grand Saint Bernard. Essai d'évaluation des critères susceptibles d'en préciser l'hérédité pré-métamorphique (Alpes valaisannes, Suisse). Thèse de doctorat, Uni Lausanne.
WERNER, C.D. (1987): Saxonian Granulites – a contribution to the geochemical diagnosis of original rocks in high metamorphic complexes. Gerlands Beiträge Geophysik, Leipzig, X, 3/4, 271–290.
WINCHESTER, J.A. and MAX, M.D. (1982): The geochemistry and origin of the Precambrian rocks of the Rossalare Complex, SE Irland. J. Geol. Soc. London, 139, 309–319.

Joel Brugger (Basel):

Mineralogy of the Iron-Manganese deposit of Fianel – Ferrera valley – Graubünden.

Fianel belongs to a group of small iron-manganese deposits embedded in the Suretta nappe cover. The ore bodies are stratiform and lenticular; they occur in different stratigraphic positions inside the Triassic carbonates that overlay the "Roffna Porphyr", a gneiss of granitic composition. The latter has numerous manganoan siderite veins that are not discussed here. Ore pebbles inside a probably Liassic breccia constrain the age of the mineralizations. The deposits were transformed by the Alpine, greenschist facies metamorphism.

The carbonate hosted deposits mainly contain iron ores; only three of them (Starlera, Fianel and Alp Tanatz by Splügen) show a substantial amount of manganese ores.

In order to understand the genesis and metamorphic evolution of these deposits, a detailed field study was undertaken in summer 1993; Fianel is the most promising locality because of the richness of its mineralogy and its relatively simple tectonic position.

Four ore facies can be distinguished in Fianel:

– Hematite quartzite ± fluorapatite (until 5 vol.%), Sr-rich barite. This is the "standard" iron ore mined in the past.

– Manganese-ore consisting of fine grained braunite, hausmannite, jacobsite ± spessartine, pyroxene, Sr-rich barite, manganite. Millimetric to centimetric veins crosscutting these lithologies contain manganoan calcite, rhodonite, parsettensite, rare kutnohorite.

Some manganoan beds (0.1 to 0.5 m thick) are highly enriched in vanadium. Medaite $(Mn,Ca)_6(V,As)Si_5O_{18}(OH)$ grows in the schistosity and gives to the rock a typical red colour. Veins inside these rocks contain an interesting vanadate asso-

ciation: palenzonaite $NaCa_2Mn_2(VO_4)_3$, saneroite $Na_2Mn_{10}VSi_{11}O_{34}(OH)_4$, pyrobelonite $PbMnVO_4(OH)$. Vanadium rich minerals from Fianel are reported for the first time.

– A "pyroxenite"-lens of about 10 × 10 × 5 meters composed to 90% by aegirine-rich pyroxene + quartz, Sr-rich barite is a unique feature of the Fianel deposit.

– The presence of beryl on the dumps of Fianel was described already by STUCKY (1960). Careful mapping of the mine allowed to find the source rock of this mineral: a metric lens of a rosy dolomite breccia with quartz-dolomite-hematite cement embedded in hematite quartzite. Quartz veins inside this rock contain beryl + F-Na-Ti-rich romeite $(Ca,Na)_2(Sb,Ti)_2O_6(F,OH,O)$ + powellite-scheelite + barite + fluorapatite, bergslagite $CaBeAsO_4(OH)$.

Strongly zoned powellite-scheelite shows a very uncommon chemistry, with more than 1 wt% As correlated with Y + REE. The REE spectrum is characterized be an enrichment in light REE (whereas scheelite usually concentrates heavy REE).

The detailed mineralogical study of the Fianel deposit reveals some typical geochemical features, that are not uncommon in metamorphic manganese deposits (e.g. Falotta/Graubünden [As–V–Sr ± Be, Sb], Langban/Sweden [V–As–Be–Sb–Sr], paleozoic Mn-deposits of the French Hautes Pyrénées [As–V–W–Be–REE]).

Most of these elements do not seem to migrate during metamorphism; no diffusion of iron in the adjacent carbonate is observed; the veins crosscutting several ore layers contain vanadates only vere they intersect a medaite-bearing-rock. Therefore it seems that when mapping the mineralogical "rarities" of Fianel which have grown during the metamorphism, we map the original pre-metamorphic geochemical situation of the deposit.

STUCKY, K. (1960): Die Eisen- und Manganerze in der Trias des Val Ferrera. Beiträge zur Geologie der Schweiz, Geotechnische Serie, 17. Lieferung.

R. Frei and M. Vinyu (Bern, Harare):

Calc-silicate alteration and associated gold mineralization at Jumbo Mine, Mazowe, Zimbabwe: U–Pb and Pb–Pb evidence for metallization at least 25 Ma later than the regional peak metamorphism.

Knowledge of the source of metal bearing fluids and their timing relative to tectonic, metamorphic and plutonic events adds some major

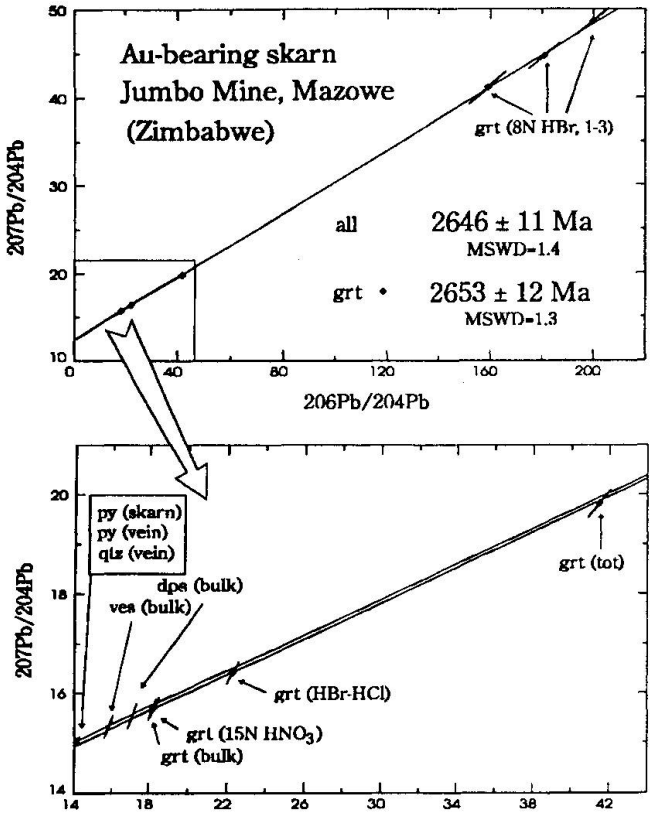

understanding to the genesis and formation of a mineral deposit. However, direct radiometric dating of mineralization events is often complicated by the lack of phases suitable for dating by the commonly applied isotope sytems (e.g. U–Pb, Rb–Sr, Sm–Nd, Ar–Ar, K–Ar). Pb–Pb analyses of ore paragenetic phases have been successfully applied to dating Au lode deposits in the Archean (e.g. CARIGNAN and GARIÉPY, 1993; JEMIELITA et al., 1990; HO et al., 1994).

We report here Pb isotope results from the Archean Jumbo Au-quartz-vein deposit (Mazowe, Harare greenstone belt, Zimbabwe), which demonstrate the potential of a powerful new leaching technique (FREI and KAMBER, 1994, subm.) applied to associated and cogenetic garnet. The Jumbo Au lode deposit is spatially related to the Proterozoic Jumbo granodiorite, dated at 2664 +16/–14 Ma (VINYU, 1993) and is structurally controlled by extensive steep E–W trending shear zones. The main reef on 18 level (18/7 Drv Nucleus) at Jumbo Mine consist of massive pyrite and quartz, in which gold mainly occurs as small (< 20 μm) blebs. The footwall consists of a porphyritic dolerite which is part of the greenstone succession. It shows an auriferous garnet-diopside-vesuvianite-calcite skarn alteration which is cogenetic with the the main reef. Field relations clearly reveal crosscutting rela-

tionships between the reef and the granodiorite, which is itself intrusive into the porphyritic dolerite.

A stepwise leaching of garnet resulted in an isochrone defining an age of 2653 ± 12 Ma (MSWD = 1.3). A Pb–Pb isochron of 2646 ± 11 Ma (MSWD = 1.4) was obtained using quartz and pyrite from the reef and garnet, diopside and pyrite from the adjoining skarn. This can be interpreted as the age of Au deposition or as complete resetting of the U–Pb system during shearing. Furthermore, it constrains the cogeneticity of vein- and alteration phases. Therefore, some gold in the Jumbo deposit has been deposited during calc silicate alteration post-dating peak metamorphic conditions and orogenic activity in the greenstone belt. In this it resembles the Hemlo gold deposit (Ontario, Canada), where PAN and FLEET (1992) report calc-silicate alteration at least 30 Ma later than peak metamorphism of the region.

CARIGNAN, J. and GARIEPY, C. (1993): Pb isotope geochemistry of the Silidor and Launay gold deposits: implications for the source of Archean Au in the Abitibi Subprovince. Econ. Geol. 88, 1722–1730.

FREI, R and KAMBER, B.S. (submitted): Pb–Pb dating of single Ca-bearig silicates; the potential of a new stepwise leaching procedure.

HO, S.E., MCNAUGHTON, NJ. and GROVES, D.I. (1994): Criteria for determining initial lead isotopic compositions of pyrite in Archean lode-gold deposits: a case study at Victory, Kambalda, Western Australia. Chemical Geology 111, 57–84.

JEMIDITA, A., DAVIS, D.W., and KROGH, T.E (1990): U-Pb evidence for Abitibi gold mineralization post-dating greenstone magmatism and metamorphism. Nature 346, 831–834.

PAN, Y. and FLEET, M.E. (1992): Calc-silicate alteration in the Hemlo gold deposit, Ontario: mined assemblages, P-T-X constraints, and significance. Econ. Geol. 87, 1104–1120.

VINDYU, M.L. (1993): Geochemistry and geochronology of the post-orogenic granitoids in the Harare-Shamva greenstone belt. Unpubl. Ph. D. Thesis, University of Zimbabwe.

G.L. Früh-Green and A. Plas (Zürich):

Hydrothermal alteration of the EPR lower crust and shallow mantle exposed at Hess deep (ODP leg 147): mineralogical and stable isotope constraints.

Sections of the fast-spreading East Pacific Rise lower crust and shallow mantle (approximately 1 Ma), tectonically exposed at the western end of the Cocos-Nazca propagator at the Hess Deep Rift Valley, were recovered for the first time during Leg 147 of the Ocean Drilling Program (ODP). These rocks record a polyphase history of hydrothermal alteration ranging from upper amphibolite facies to zeolite facies conditions and provide new constraints on the depth and mechanisms of hydrothermal circulation at fast-spreading ridges. At Site 894, approximately 150 m of variably metamorphosed, isotropic gabbros and gabbronorites from the upper part of the plutonic section were drilled. Early amphibolite-facies mineral assemblages occur in microveins and along grain boundaries, and include Ca–Al amphibole, diopsidic clinopyroxene, calcitic plagioclase, ilmenite and magnetite. Variable overprinting under transitional amphibolite-greenschist to zeolite facies conditions is characterized by the occurrence of actinolitic amphibole, Na-plagioclase, and smectite, with minor chlorite, calcite, K-feldspar and zeolites. These lower temperature assemblages are associated with discrete macroscopic veins and local cataclastic shear zones related to the propagation of the Cocos-Nazca rift.

A complex sequence of upper mantle harzburgites cut by dunite, which often enclose mafic sequences of troctolite, olivine gabbro and gabbro, were recovered at Site 895. The harzburgite-dunite-gabbro association and the relative abundance of dunite are considered to result from processes of melt migration, wall-rock reaction and cumulus olivine precipitation close to the mantle-crust boundary. The peridotites are extensively serpentinized (50–100%) and are cut by multiple generations of fracture-filling veins. Greenschist to zeolite facies alteration and incipient rodingitization of the gabbroic rocks is indicated by tremolite + chlorite + anorthite ± prehnite assemblages in the least altered samples, with increasing proportions of hydrogrossular, zeolites and clays as cataclastic deformation increases.

Oxygen isotope ratios of mineral separates of the gabbros and peridotites from both sites show a depletion in ^{18}O relative to mantle values and are consistent with high temperature exchange with aqueous fluids. Only the plagioclase in the high level gabbros at Site 894 deviate from this general trend and show a bimodal distribution, consisting of a high temperature altered group with $\delta^{18}O$ between 3.0 and 6.3‰ and a group with $\delta^{18}O$ between 8.3 and 10.2‰ indicative of local lower temperature overprinting associated with discrete veining. Hydrogen isotope ratios of chlorite, serpentine and amphibole suggest two components of the hydrothermal fluids: a hydrothermally altered seawater component (with δD close to 0‰) and a mixed magmatic-derived/altered seawater component (with δD 20 to 3‰ lighter than seawater). Petrological and stable

isotope data, combined with structural data suggests that penetration of seawater at high temperatures (> 300 °C), mixing with magmatic fluids and hydrothermal circulation at Hess Deep was controlled by the Cocos-Nazca rifting at an early stage, producing a low ^{18}O sequence of oceanic lithosphere early in the spreading history of the EPR.

V. Gardien, E. Reusser and D. Marquer
(Lyon, Zürich, Neuchâtel):

Compared P,T evolutions between paleo (Valpelline series) and actual (Galicia Spain) continental margins.

High temperature (800–1000 °C) granulites associated with mafic and utltramafic rocks are interpreted as lower crust/ upper mantle sections metamorphosed under high geothermal regime during a thinning event and following tectonical uplift. The Valpelline series of the Dent Blanche nappe (Western Alps) is one of such examples. One possibility to test this working hypothesis is to precise the metamorphic conditions for both crustal and mantle rocks in an actual continental passive margin, the Galicia Margin (western Spain).

At the boundary between the thinned crust of the Galicia margin and the oceanic crust of the Atlantic, the basement beneath the sediments form a ridge which consists of serpentinized peridotites (plagioclase bearing harzburgites and lherzolites) (BOILLOT et al., 1986; BESLIER et al., 1988; EVANS and GIRARDEAU, 1988; KORNPROBST and TABIT, 1988). The peridotites experienced a succession of structural and metamorphic events: an early partial melting event (5–9%) at shallow depth (< 30 km) and high temperature (1250–1000 °C) which implies asthenospheric diapirism (GIRARDEAU et al., 1988). Later the peridotites underwent ductile deformation by simple shear (BESLIER et al., 1988) dated at 122 Ma (FÉRAUD et al., 1988). Finally the rock was hydrothermally altered to serpentinite and fractured at the end of the rifting (before 114 Ma). The crustal continental rocks adjacent to the peridotite ridge are for the most part alkaline granites, granodiorite and some syenites. Micro structural and petrologic investigations show that most of this rocks have been deformed under ductile conditions at low pressure (54 kbar) and high temperature (700–750 °C) conditions coherent with the P-T conditions recorded by mantle rocks.

Both Valpelline and Arolla series comprise the Dent Blanche nappe which is believed to belong to the southern (African) continental margin during Jurassic time. The main lithologic units of the Valpelline series consist of metapelites, mafics and carbonates. In the metapelites we observe porphyritic inclusion-rich garnets rimmed by a layer of inclusion-free garnet. The inclusions are mainly K-feldspar, quartz, rutile, plagioclase, kyanite and biotite. They appear oriented but not in the same plane as the present foliation indicating that garnets have grown previously. The matrix is composed of quartz, plagioclase ilmenite, biotite and sillimanite elongated within the present foliation with relics of kyanite and rutile. Microstructural and petrological investigations allow two metamorphic stages to be deciphered. The first one is an intermediate pressure granulitic stage 8–10 kbar and 600–700 °C. The retrograde stage under LP-HT granulitic facies conditions 5–6 kbar and 750–800 °C associated to the development of asymmetric shear bands and mylonitic foliation.

The comparison between P-T evolution in crustal and mantle rocks from the Valpelline series and the Galicia margin is designed to elucidate the thermal regime occurring in the crust during the rifting stage of passive margin.

BOILLOT, G., COMAS, M.C., GIRARDEAU, L., KONNPROBST, J., LOÉREAU, J.P., MALOD, J., MOUGENOT, D. and MOULLADE, M. (1986): Fonds sous-marins basaltiques et ultramafiques au pied d'une marge stable. Résultats préliminaires de la campagne Galinaute. C.R. Acad. Sci. Paris, II, 203, 1719–1724.

BESLIER, M.O, GIRARDEAU, J. and BOILLOT, G. (1988): Lithologie et structure des péridotites à plagioclase bordant la marge continentale passive de la Galice (Espagne). C.R. Acad. Sci. Paris, II, 373–380.

EVANS, C.A. and GIRARDEAU, J. (1988): Low-temperature alteration of peridotites, Hole 637A. In BOILLOT, E.L. et al. (eds): Proc. ODP. Sci. Results. 103, 235–239.

GIRARDAU, J., EVANS, C.A. and BESLIER, M.O. (1988): Structural analysis of plagioclase-bearing peridotites emplaced at the end of the continental rifting. Hole 637A. In BOILLOT, E.L. et al. (eds): Proc. ODP. Sci. Results. 103, 209–223.

FÉRAUD, G., GIRARDEAU, G., BESLIER, M.O. and BOILLOT, G. (1988): Datation $^{39}Ar/^{40}Ar$ de la mise en place des péridotites bordant la marge de Galice (Espagne). C.R. Acad. Sci. Paris. II, 49–55.

KORNPROBST, J. and TABIT, A. (1988): Plagioclase-bearing ultramafic tectonites from the Galicia margin (leg 103, site 637): comparison of their origin and evolution with low-pressure ultramafic bodies in western Europe. In BOILLOT, E.L. et al. (eds): Proc. ODP. Sci. Results. 103, 253–263.

W. Hansmann, M. Maggetti and V. Köppel
(Zürich, Fribourg):

Comparison of Pb isotope with trace element signatures of polymetamorphic rocks from the Silvretta nappe.

Within the Austroalpine Silvretta nappe MAGGETTI et al. (1990) distinguish four major groups of crystalline rocks: (1) Paragneisses, (2) eclogites and amphibolites, (3) older orthogneisses and (4) younger orthogneisses. The paragneisses comprise biotite-plagioclase-gneisses and micaschists. They are closely associated with MORB-type eclogites and amphibolites which were derived from tholeiitic protoliths. Their geotectonic setting could correspond either to an advanced stage of rifting of a continental plate or to a divergent oceanic plate boundary that was located close to a continent which provided detrital input. These rocks were metamorphosed under amphibolite facies conditions and were subsequently intruded by the older orthogneisses which include ultramafic, gabbroic, dioritic to quartzdioritic and granitic rocks. The basic and intermediate members of this suite exhibit I-type characteristics whereas the granitic members are of S-type origin. A second period of metamorphism preceeded the intrusion of the younger, approx. 450 Ma old orthogneisses which comprise a variety of augengneisses and also show S-type signatures. The majority of the intermediate and granitic members of both, older and younger orthogneisses, are related to volcanic arcs.

Lead isotope analyses were performed on mineral separates from rocks of the four major groups. In spite of the polymetamorphic history the isotope signatures reveal a spectrum ranging from mantle-type lead (low $^{207}Pb/^{204}Pb$ relative to $^{206}Pb/^{204}Pb$) to high μ crustal lead (high $^{207}Pb/^{204}Pb$ relative to $^{206}Pb/^{204}Pb$, data points close to or above the gowth curve [Fig. 1]). In situ decay of U shifted the data points towards higher radiogenic values, but the slope of the tie lines of mineral pairs corresponds in most cases to the slope of the growth curve (Fig. 1) in Phanerozoic times.

The paragneisses contain a high-μ lead which indicates a long residence time of the lead in a relatively U-rich environment. This signature is typically observed in paragneisses of the Austroalpine nappes and of the Southern Alps. Within the amphibolite-eclogite group a strong mantle component is present in the amphibolite whereas the eclogite displays an average crustal Pb signature. The lead of basic members of the group of older orthogneisses contains a more or less distinct mantle component, whereas the lead of granitic rocks is of average crustal composition. The younger augengneiss shows a Pb composition that is rather similar to the one observed in paragneisses. The lead isotope data thus supports in most cases the interpretation of the geochemical signatures. The data of metaigneous rocks indicates an increasing cratonization of the Silvretta basement with time.

MAGGETTI, M, FLISCH, M. and BOLLIN, R. (1990): Bericht über die Exkursion der Schweiz. Mineralogischen und Petrographischen Gesellschaft ins Silvretta-Kristallin und in den Westrand des Unterengadiner Fensters (11.–14. September, 1989). Schweiz. Mineral. Petrogr. Mitt. 70, 121–157.

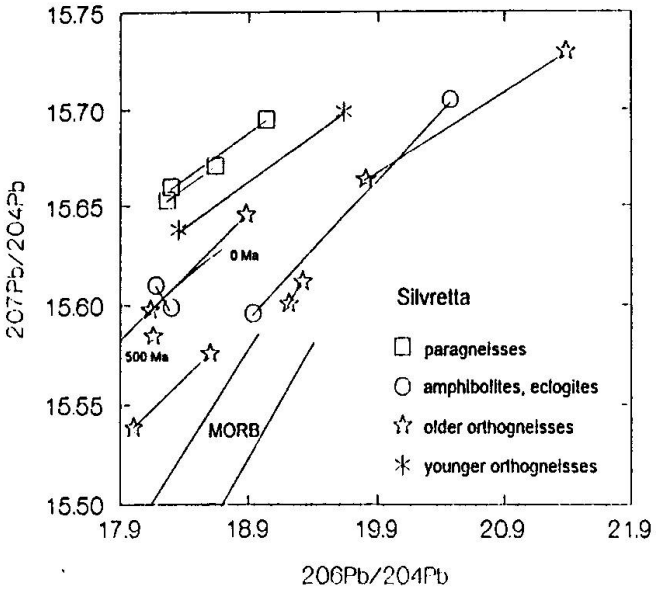

Fig. 1 Uranogenic Pb-isotope evolution diagram. Data points of mineral pairs are connected by tie lines. Present-day MORB data field and growth curve from 500 to 0 Ma are shown.

L. Holzer, B. Kamber and J. Kramers (Bern):

The dissection of a supposedley Archean example of continent-continent collision: the Limpopo Belt of southern Africa.

The Limpopo Belt lies between two Archean cratons: the Kaapvaal craton in the south and the Zimbabwe craton in the north. It consists of three tectonic units: the northern and southern marginal zones (NMZ and SMZ) and the central zone (CZ). *The marginal zones* are the high grade equivalent of granite-greenstone terranes. The contacts to the adjacent cratons are reverse faults. Therefore the marginal zones are considered as equivalents of the lower crust of the adjacent cratons. The metamophic grade increases from greenschist to granulite facies towards the central zone. *The central zone* is bounded by the dextral Triangle shear belt in the north (> 50 km wide) and the sinistral Palala shear zone in the south. The lithologies of the CZ are different from those of the marginal zones: On an early

Archaen basement thick sequences of sediments were deposited. Several intrusions of granites, mafic dykes and ultramafic bodies took place over a wide time span in the Archean. The CZ was metamorphosed several times and shows granulite facies parageneses.

The model "Limpopo orogeny" describes an Archaen continent-continent collision between the Kaapvaal and the Zimbabwe cratons at 2.65 Ga. The Limpopo Belt is considered as the product of this tectonometamorphic event (ROERING et al., 1992; BARTON and VAN REENEN, 1992; LIGHT, 1982). The symmetry of the structures (reverse faults between cratons and marginal zones, CZ as escaping block bounded by shear belts) as well as the symmetry of the lithologies (marginal zones as lower crust equivalents of the adjacent cratons, CZ as exothic terrane in between) are main arguments to consider the Limpopo as an orogenic belt. It is suggested that major tectonometamorphic activity in the whole belt is of the same age, because granitic bodies that are interpreted as syntectonic intrusions yield ages around 2.65 Ga. (e.g. Matok in SMZ, Bulai in CZ, Razi in NMZ). All metamorphic analysis show clockwise p-T-t paths (e.g. STEVENS and VAN REENEN, 1992; DROOP, 1989).

New geochronological data lead to *the dissection of this model:* parts of the NMZ and CZ underwent *granulite facies metamorphism and intense deformation at 2.0 Ga* (KAMBER et al., in press; BARTON et al., in press; HOLZER, unpubl. data). KAMBER et al. could also show that the Triangle shear belt was active under high grade conditions at 2.0 Ga. In contrast the Palala shear zone was active under high grade conditions probably at about 2.65 Ga. This shear zone was reactivated under low grade conditions at 2.0 Ga, crosscutting the Bushveld intrusion. With these new data the arguments for a continent-continent collision considering structural and metamorphic symmetry and simultaneity (as described above) are invalid.

U–Pb zircon dating of the Bulai intrusion in the CZ gives an age of 2.57 Ga (BARTON et al., in press). It is therefore 80 Ma younger than the postulated Limpopo orogeny. The multiple phase deformation in the Bulai Gneiss and also the last deformational phases in the country rock (e.g. Sandriver-Gneisses) are products of the tectonometamorphic event at 2.0 Ga.

Garnets from Bandelierkop Quarry (SMZ) yield ages of 3.1 Ga (BARTON et al., in press). Therefore the PTt path described by STEVENS and VAN REENEN (1992) most probably mixes data from parageneses which equilibrated during different metamorphic events. All these new data lead to the conclusion that *there is no simple large Archean Limpopo Orogeny*. Even though granulite parageneses are found in the marginal zones as well as in the CZ, granulite facies conditions are not simultaneous: The northern part of the CZ and the NMZ yield high grade conditions at 2.0 Ga. At this time the SMZ was already under low grade conditions. The apparent symmetry of the Limpopo Belt is the product of several tectonic movements at different times: The tectonic units Kaapvaal craton, SMZ and CZ were juxtaposed during the Archean. This whole block was brought to its final position relative to NMZ and Zimbabwe craton at 2.0 Ga, when the Triangle shear zone was active. Petrographical analysis and geochronological data indivate rapid uplift of CZ and NMZ before 1.95 Ga.

The new data clearly show that it is unwise to use syntectonic intrusions as time markers, because the information about synintrusive metamorphic conditions is weak. PTt models which mix geochronological data from intrusive bodies with thermobarometric data from other lithologies and localities across tectonic boundaries may lead to misinterpretations.

BARTON, J.M., JR. and VAN REENEN, D.D. (1992): When was the Limpopo Orogeny? Prec. Res., 55, 7–16.

BARTON, J.M., JR., HOLZER, L., KAMBER. B., DOIG, R., KRAMERS, J.D. and NYFELER, D. (1994): Discrete metamorphic events in the Limpopo Belt: Implications for the interpretation of P-T-t paths in metamorphic terrains. Geology (in press).

DROOP, G.T.R. (1989): Reaction history of garnet-sapphirine granulites and conditions of Archaean high-pressure granulite-facies metamorphism in the Central Limpopo Mobile Belt. Zimbabwe. J. metamorphic Geol., 7, 383–403.

KAMBER, B., KRAMERS, J.D., NAPIER, R., CLIFF, R.A. and ROLLINSON, H.R. (1994): The Triangle shear zone, Zimbabwe, rovtsited: what remains of the Archean Limpopo Orogeny. Proc. Res. (in press).

LIGHT, M.P.R. (1982): The Limpopo Mobile Belt: a result of continental collision. Tectonics, 1, 325–342.

ROERING, C., VAN REENEN, D.D., SMIT, C.A., BARTON, J.M., DE BEER. J.H., DE WITT, M.J., STETLER, E.H., VAN SCHALKWYK, J.F., STEVENS, G. and PRETORIUS, S. (1992): Tectonic model of the evolution of the Limpopo Belt. Prec. Res., 55, 539–552.

STEVENS, G. and VAN REENEN, D.D. (1992): Constraints on the form of the P-T loop in the SMZ of the Limpopo Belt. Prec. Res., 55, 279–296.

M. Krzemnicki (Basel):

REE-haltige Arsenite und Arsenate aus der Monte Leone-Decke (Binntal, Schweiz).

REE-bearing arsenites and arsenates from the Monte Leone nappe (Binntal, Switzerland).

Die Monte Leone-Decke (ML-Decke) ist bekannt für ihre aussergewöhnlichen Mineral-lagerstätten; das Sulfosalz-Vorkommen im Dolomitaufschluss beim Lengenbach und die hydrothermale Arsen-Minerallagerstätte im Kristallin der ML-Decke.

Diese Arbeit untersucht die Mineralchemie der komplexen Arsenoxide, welche in alpinen Zerrklüften im ML-Gneis der Binntal-Region vorkommen. Bedingt durch die rasche Hebung der penninischen Einheiten gegen Ende der alpinen Orogenese kam es zu einer sehr intensiven hydrothermalen Aktivität, welche die präalpinen sulfidischen As-, Cu-, Bi-, Seltene Erden Elemente (REE)-Lagerstätten remobilisierte (GRAESER and ROGGIANI, 1976). Die angereicherten Hydrothermen migrierten bevorzugt entlang diskreter Brüche innerhalb der ML-Decke.

Mit der Elektronen-Mikrosonde wurden an einer ganzen Reihe von *Arseniten* (Cafarsite, Asbecasite) und *Arsenaten* (Agardit-[Y]) von verschiedenen Fundorten innerhalb des ML-Gneises detaillierte qualitative und quantitative Analysen vorgenommen. In allen untersuchten Cafarsiten und Asbecasiten wurden REE (La, Ce, Nd, Y) nachgewiesen (bis zu 2 Gew.% REE_2O_3). Anhand von Korrelationsdiagrammen scheint bei beiden Arseniten dieselbe gekoppelte Substitution wirksam gewesen zu sein:

$Ca^{2+} + Ti^{4+} \leftrightharpoons REE^{3+} + Fe^{3+}$.

HEINRICH und EADINGTON (1986) berechneten ein thermodynamisches Modell mit As-Hydroxid-Komplexen bei metamorphen Bedingungen. Dies ist das grundlegende Modell, um den hydrothermalen Transport von Arsen in der ML-Decke zu verstehen. Obwohl die REE früher allgemein als relativ immobile Elemente bezeichnet wurden, haben verschiedene neue Untersuchungen gezeigt, dass die Mobilität der REE in hydrothermalen Fluids stark erhöht ist, wenn diese Komplexe mit F^-, Cl^-, CO_2 und möglicherweise auch reduzierten Schwefel-Spezies, z.B. H_2S, HS^- und S^{2-} (CULLERS and GRAF, 1984; GIERÉ, 1993) formen.

Aufgrund der Anwesenheit von Fluorit, Fluorapatit und Mimetesit scheinen die F^- und Cl^--Komplexe hauptsächlich verantwortlich für den hydrothermalen Transport der REE innerhalb der ML-Decke. Aber auch H_2S, als wichtigster Lösungs-Agens der primären As-Sulfide (Tennantit und ± Arsenopyrit), mag eine wichtige Rolle für die REE-Mobilisation gespielt haben. Die offensichtliche, enge Vergesellschaftung von REE mit Arsen könnte ein Hinweis darauf sein, dass die REE auch Komplexe mit $(AsO_3)^{-3}$ bildeten.

Die REE-haltigen As-Mineralien im ML-Gneis sind Oxidationsprodukte einer alpin remobilisierten, präalpinen As-Cu-Sulfid-Lagerstätte. Bei zunehmender Sauerstoff-Fugazität in der ML-Decke während der alpinen Metamorphose kam es zuerst zur Ausscheidung der REE-haltigen Arsenite in den Zerrklüften und in einer zweiten Phase zur Kristallisation der ± REE-haltigen Arsenate in unmittelbarer Nachbarschaft zu den zersetzten Arseniten.

CULLERS, R.L. und GRAF, J.L. (1984): Rare Earth Elements in igneous rocks of the continental crust: Intermediate and silicic rocks. Elsevier, Developments in Geochemisty, Nr. 2, 300–316.

GIERÉ, R. (1993): Transport and deposition of REE in H_2S-rich fluids: exvidence from accessory mineral assemblages. Chem. Geol. 110, 251–268.

GRAESER, S. und ROGGIANI, A.G. (1976): Occurrence and genesis of rare arsenate and phosphate minerals around Pizzo Cervandone, Italy/Switzerland. Rend. Soc. Ital. Min. Petrogr. 32, 279–288.

HEINRICH, C.A. and EADINGTON, P.J. (1986): Thermodynamic predictions of the hydrotherrnal chemistry of arsenic, and their significance for the paragenetic sequences of some Cassiterite-Arsenopyrite-base metal Sulfide deposits. Econ. Geol. 81, 511–530.

V. Liebetrau, U. Poller, S.A. Sergeev and R. Frei (Fribourg, Zürich, Bern):

Contradictory U–Pb zircon data of S-type grantoids (Silvretta nappe) in consideration of CL supported interpretation.

The complex zircon U–Pb data for S-type granitoids in the Austroalpine Silvretta nappe called for a detailed study of the internal morphology of the zircons. A cathodoluminescence (CL) investigation was initiated which revealed the internal zircon structures and greatly aided in the interpretation of the data set.

The following three clear zircon morphologies were found to be present in the population of each rock sample: 1. prismatic type, 2. bipyramidal type and 3. flattened species. For one granitoid type (Mönchalp gneiss) the analyses of three different typological populations within the same size fraction suggest a discordia line with a lower intercept around 460 Ma. Bipyramidal single grains considered as last magmatic, result in discordant data points which differ in age because of an optically invisible inherited component. But their combination with other grain size fractions leads to a discordia with an apparent lower intercept of 510 Ma. Upper intercept ages of both discordias indicate an inherited 2.3 Ga old Pb component. In contrast to this, the single-grain data of an other orthogneiss (Urezzas) give concordant points around 450 Ma.

CL imaging by scanning electron microscope show that among (magmatic) zoned grains of the same typology and size there exist some which bear inherited cores of which at least three types may be distinguished: 1. a conglomerate of several small cores, 2. broken (detrital) well structured cores and 3. weakly structured resorbed cores. Grains bearing one of the first two core types, often exhibit parts of diffuse growth structures between core and rim.

Correlated with the S-type characteristics of the rocks and the metamorphic and magmatic evolution of the Silvretta nappe (MAGGETTI and FLISCH, 1993) the controversy discordia ages can be reinterpreted in consideration of the internal zircon structures. The problems for the different methods including single grain zircon dating, multi grain analyses and Pb–Pb evaporation technique can be explained by CL interpretation.

A special preparation technique, which allows CL investigation and dating of the same zircon crystal, would offer the possibility to utilize the different advantages of each dating method. In summary the combination of these procedures gives an important tool to solve the polyphase history of S-type granitoids.

MAGGETTI, M. and FLISCH, M. (1993): Evolution of the Silvretta Nappe, In VON RAUMER, J.F. and NEUBAUER, F. (eds): Pre-Mesozoic Geology in the Alps, Springer Berlin, 469–484.

M. Maggetti and G. Galetti (Fribourg):

Magmatic evolution and geotectonic setting of the Silvretta amphibolites.

The Silvretta nappe contains the highest amount (ca. 30%) of amphibolites in the crystalline units of the Alps. We have analyzed more than 200 samples which were collected statistically over the whole Silvretta. The amphibolites s.l. comprise plagioclase-amphibolites (which are the dominant lithology), garnet amphibolites, and spotted amphibolites. These rocks are often associated with hornblende rocks/actinolitic felses (more than 90 vol.% amphibole). The amphibolites s.l. (meta-mafites) and the hornblende rocks/actinolitic felses (meta-ultramafitites) are typically hosted by paragneisses (meta-greywackes to meta-pelites). In the field, all transitions between eclogites, symplectitic garnet-amphibolites, garnet-amphibolites and plagioclase amphibolites can be observed. It suggests that all amphibolites s.l., as well as the meta-ultramafitites underwent high pressure metamorphism.

Based on the usual classification diagrams, the amphibolites s.l. belong to Mg-tholeiites, normal tholeiites and Fe-tholeiites; the meta-ultramafitites to komatiitic basalts. The chemical composition of the amphibolites s.l. suggests that they derived from evolved tholeiitic magmas which have undergone variable degrees of fractionation at shallow levels involving crystallization of plagioclase + olivine + pyroxene + spinel. The igneous protoliths (basalts and gabbros) were formed by crystallization from tholeiitic MORB-like liquids at spreading ridges after continental break-up or in marginal basins, close to a continent. The whole series resemble the meta-basaltic and meta-ultramafic suite described by STILLE and TATSUMOTO (1985).

STILLE, P. and TATSUMOTO, M. (1985): Precambrian tholeiitic dacitic rock-suites and Cambrian ultramafic rocks in the Penninic nappe system of the Alps: evidence from Sm–Nd isotopes and rare earth elements. Contrib. Mineral. Petr. 89, 184–192.

Ch. Meyre, J.H. Partzsch, M. Frey, S.M. Schmid und C. De Capitani (Basel):

Die metamorphe Entwicklung der mittleren Adula-Decke (Zentralalpen, Schweiz).

Metamorphic evolution of the Adula nappe (Central Alps, Switzerland).

Die Adula-Decke, die im penninischen Deckenstapel der östlichen Zentralalpen eine tiefe tektonische Stellung einnimmt, wird von vier alpinen Deformationsphasen (D1–D4) geprägt. Sie weist, im Gegensatz sowohl zu der Tambo-Decke im Hangenden als auch zu der Simano-Decke im Liegenden, eine alpine, eklogitfazielle Metamorphose auf. Relikte dieser Metamorphose sind auf das Hangende der Adula beschränkt (HEINRICH, 1986).

Internstrukturen der Eklogite (Foliation sowie Streckungslinear, abgebildet durch dynamisch rekristallisierten Omp und Grt-Aggregate) können der ersten Deformationsphase D1 zugeordnet werden. Die zweite Deformationsphase verfaltet unter eklogitfaziellen Bedingungen (D2a; MEYRE und PUSCHNIG, 1993) die basischen Lagen und geht nahtlos in D2b (amphibolitfaziell) über. D2b ist verantwortlich für die retrograde Überprägung der Eklogite, die Ausbildung der Hauptschieferung und des Streckungslinears L2. D2b-Strukturen können bis in die Misoxer Zone verfolgt und mit der Ferrera-Phase der Schamser Decken (SCHMID et al., 1990) korreliert werden. Dies weist auf eine gemeinsame tektonische Entwicklung der Adula-Decke mit den

penninischen Decken im Hangenden hin. Die Überschiebung der Adula-Decke auf die Simano-Decke findet erst während D3 statt (PARLZSCH et al., 1994). Im Top der Adula-Decke äussert sich D3 in offenen Falten sowie der Ausbildung einer Crenulation in den Metapeliten. D4 zeigt sich in einer Wellung und Knickung der Gneise und Metapelite im Übergangsbereich zwischen Duktil- und Spröddeformation.

Die Mineralchemie der Granate eines stark deformierten Eklogits von Confin zeigt eine prograde Entwicklung: Prä-eklogitfazielle, xenomorphe Granat-Kerne werden überwachsen von eklogitfaziellen, idiomorphen Granaten, die deutlich zoniert sind. Die Omphazite sind dynamisch rekristallisiert und chemisch homogen. Sie besitzen identische Zusammensetzungen wie Omphazite, die in Granat-Druckschatten von einer Rekristallisation verschont blieben. Geothermometrie anhand des Fe-Mg-Austauschgleichgewichts zwischen Klinopyroxen und Granat (z.B. KROGH, 1988) weisen auf Temperaturen von ca. 550 °C bei 15 kbar hin. Für Eklogite der südlich gelegenen Alp d'Arbeola lassen sich Bedingungen von 600–650 °C bei leicht höheren Drucken (18 kbar) berechnen. Thermodynamische Berechnungen von Phasengleichgewichten liefern übereinstimmende Resultate.

Das Alter der eklogitfaziellen Metamorphose ist noch umstritten, jedoch lässt die kontinuierliche Entwicklung der Deformationsphasen ab D2a (eklogitfaziell) einen tertiären Höhepunkt als möglich erscheinen.

HEINRICH, C.A. (1986): Eclogite facies regional metamorphism of hydrous mafic rocks in the Central Alpine Adula nappe. J. Petrology, 27, 123–154.

KROGH, E.J. (1988): The garnet clinopyroxene Fe–Mg geothermometer – a reinterpretation of existing experimental data. Contrib. Mineral. Petrol., 99, 44–48.

MEYRE, C. und PUSCHNIG, A. R. (1993): High-pressure metamorphism and deformation at Trescolmen, Adula nappe, Central Alps. Schweiz. Mineral. Petrogr. Mitt., 73, 277–283.

PARTZSCH, J.H., FREY, M., KRUSPAN, P., MEYRE, C. und Schmid, S.M. (1994): Die tektono-metamorphe Entwicklung der mittleren Adula-Decke (Zentralalpen, Schweiz). 5. Symposium Tektonik – Strukturgeologie – Kristallingeologie. Göttinger Arb. Geol. und Paläont., Sbl., 124–126.

B. Müller and M. Flisch (Zürich, Bern):

Cadomian U/Pb zircon age and Rb/Sr data of Val Sarsura garnet-hornblende-plagioclase gneisses, Silvretta Nappe, Eastern Alps, and a model for their origin.

Val Sarsura *garnet-hornblende-plagioclase gneisses* yield a Cambrian, preliminary U/Pb zircon Concordia upper intercept age of 520 ± 32 Ma. It is interpreted as the crystallization age of its igneous precursor and is in good agreement with previous age determinations of "older orthogneisses" in the nappe (MÜLLER et al., 1994). Initial ε_{Nd} of + 5.6 indicates mantle origin for ga-hbl-plag-gneisses. Their initial $^{87}Sr/^{86}Sr$ values of 0.7062 to 0.7072 are explained by radiogenic Sr supply possibly due to metamorphisms. Geochemically related *gabbronorites and flasergabbros* yield an isochron with an age estimate of 593 ± 18, which appears too high for geological reasons. A $^{87}Sr/^{86}Sr$ intercept of 0.7036 conforms to the depleted mantle origin as postulated by MAGGETTI, GALETTI and STOSCH (1990). Initial $^{87}Sr/^{86}Sr$ ratios of *ultramafic* rocks is approx. 0.7027 (calculated for 520 Ma) indicating depleted mantle origin as well. All three rock types yield whole rock isotope ratios interpretable in terms of mantle origin. Their close petrographic and isotope geochemical association indicates a common magmatic source.

REE contents and patterns (MAGGETTI, GALETTI and STOSCH, 1990) as well as main oxides and ε_{Nd} of garnet-hornblende-plagioclase gneisses are consistent with an oceanic plagiogranite (COLEMAN and PETERMAN, 1975) protolith. The ga-hbl-plag-gneiss protoliths could have had close relations to gabbroic and ultramafic rocks: the positive Eu anomaly of ultramafic rocks may result from accumulated plagioclase, in contrast to the negative Eu anomaly found in the ga-hbl-plag gneisses. On the other hand, the negative Eu-anomaly of the garnet-hornblende-plag-gneisses is traced to the positive anomaly in plag. Anorthosite layers are frequent in ophiolitic complexes. The high REE content of ga-hbl-plag-gneisses is probably the result of settling of the relatively REE-poor ol, pyx and plag, concentrating the REE in the interstitial magma. We presume that ultramafic rocks are the cumulates of fractional crystallization, that led in its final stages to the precursors of ga-hbl-plag-gneisses. A basic magma with a flat REE pattern could have been the primitive source for the whole suite. Generation of flasergabbros was slightly different. KAY and SENECHAL (1976), interpreted oceanic trondhjemites from the Troodos ophiolite complex in the same way. They stressed out the positive Eu-anomalies in peridotites vs negative Eu-anomalies in trondhjemites of that suite. Such oceanic rocks indicate a local oceanization in the Upper Austroalpine realm.

COLEMAN, R.G. and PETERMAN, Z.E. (1975): Oceanic Plagiogranite. J. Geophys. Res. 80, 1099–1108.

KAY, R.W. and SENECHAL, R.G. (1976): The Rare Earth

Geochemistry of the Troodos Ophiolite Complex. J. Geophys. Res. 81, 964–970.
MAGGETTI, M., FLISCH, M. and BOLLIN, R. (1990): Bericht über die Exkursion der Schweiz. Mineralogischen und Petrographischen Gesellschaft ins Silvrettakristallin und in den Westrand des Unterengadiner Fensters. Schweiz. Mineral. Petrogr. Mitt. 70, 121–157.
MAGGETTI, M., GALETTI, G. and STOSCH, H.G. (1990): Geochemische Argumente zur Genese der "Älteren Orthogneise" der Silvretta. Schweiz. Mineral. Petrogr. Mitt. 70, 103–107.
MAGGETTI, M. and FLISCH, M. (1993): Evolution of the Silvretta Nappe. In VON RAUMER, J.F. and NEUBAUER, F. (eds): Pre-Mesozoic Geology in the Alps. Springer, Berlin Heidelberg New York.
MÜLLER, B., KLÖTZLI, U. and FLISCH, M. (1994): Dating of the Silvretta Older Orthogneiss intrusion: U-Pb-Zircon data indicate Cadomian magmatism in the Upper Austroalpine realm. Schweiz. Mineral. Petrogr. Mitt. 74, 296–297.

R. Mundil, P. Brack, M. Meier and F. Oberli (Zürich):

Hochauflösende U-Pb-Altersdatierungen an Einzelzirkonen zur Kalibration der triassischen Zeitskala und Periodizitäten von Plattform-Karbonatzyklen der Südalpen.

Calibration of the Triassic time scale by high resolution U–Pb dating of single zircons and periodicity of platform carbonate cycles of the Southern Alps.

Mitteltriassische Karbonatplattformen der Dolomiten weisen auffallende Zyklizitäten mit Milankovitch-Charakteristik auf (GOLDHAMMER et al., 1987). Unter Berufung auf Spektralanalysen postulieren die Autoren hochfrequente Meeresspiegelschwankungen unter Einfluss des 20-ka-Präzessionszyklus als Ursache der Zyklizitäten. Die Überlagerung eines asymmetrischen 100-ka-Exzentrizitätszyklus soll die charakteristische Fünferbündelung der Schichten erklären.

Bei einer Anzahl von ca. 600 Zyklen im Präzessionsspektrum würde sich für das Wachstum der Latemar-Plattform vom Oberanis bis Mittelladin eine Dauer von mindestens 12 Ma ergeben. Dies war bis dato jedoch nicht durch absolute Altersbestimmungen belegt und steht im Widerspruch zu gängigen Zeitskalen. Dennoch gelten die Latemar-Zyklen als klassisches Beispiel für Milankovitch-Periodizitäten in der Trias.

Die Plattformkarbonate lassen sich mit altersgleichen pelagischen Abfolgen ("Buchensteiner Schichten") sowohl biostratigraphisch als auch mit Hilfe der Plattform-Becken-Geometrie korrelieren. Insbesondere Ammonoideen und Daonellen erlauben eine präzise Korrelation von Plattform- und Beckensedimenten (BRACK und RIEBER, 1993).

Vulkanoklastische Einschaltungen (Pietra Verde) in den Buchensteiner Schichten erstrecken sich über einen Zeitraum vom Oberanis bis Oberladin und ermöglichen durch das Vorhandensein von Zirkonen und anderen U-Th-führenden Mineralen die Bestimmung radiometrischer Alter. Darüber hinaus dienen charakteristische Abfolgen von Tuffhorizonten neben den Fossilien zur Korrelation der pelagischen Abfolgen, die sich über den gesamten südalpinen Raum bis hin zum Balaton-Hochland in Ungarn erstrecken. Tuff- und Bentonithorizonte aus biostratigraphisch dokumentierten Profilen am Monte San Giorgio, aus den Brescianer Alpen, den Dolomiten und dem Balaton-Hochland wurden beprobt.

Bei der Probenaufbereitung wurden nach Separation der schwersten Mineralfraktion Zirkone ausgewählt und dokumentiert. Einzelkristalle bis 500 µm Länge wurden im Durchlichtmikroskop analysiert und potentiell Altbestand führende Körner ausgeschlossen (OBERLI et al., 1989). Um konkordante Datenpunkte zu erhalten, wurde der Einfluss sekundären Bleiverlustes durch mechanische Abrasion der Mineraloberflächen minimiert.

Bis dato konnten drei vulkanoklastische Horizonte aus Profilen der Brescianer Alpen und der Dolomiten präzis datiert werden. Für den stratigraphisch ältesten Horizont aus der *Protrachyceras gredleri-Zone (Profil* von Bagolino, Brescianer Alpen) ergibt sich ein mittleres $^{206}Pb/^{238}U$-Alter von 238.8 ± 0.4 Ma (95% c.l. ext.) aus vier konkordanten U-Pb-Analysen. Aus dem gleichen Profil definieren Zirkone eines jüngeren Horizontes *(Protrachyceras archelaus-Zone)* ein mittleres $^{206}Pb/^{238}U$-Alter von 237.7 ± 1.2 Ma. Für die jüngste Pietra Verde-Lage im Seceda-Profil (Dolomiten), ebenfalls aus der *Protrachyceras archelaus-Zone*, resultiert ein mittleres $^{206}Pb/^{238}U$-Alter von 237.3 ± 0.8 Ma.

Unter Berücksichtigung des maximalen Fehlers erhält man zwischen der ältesten und der jüngsten datierten Lage ein Zeitintervall von maximal 2.7 Ma. Werden für die pelagischen Knollenkalke der Buchensteiner Schichten annähernd konstante durchschnittliche Sedimentationsraten angenommen, dauert das plattformäquivalente Zeitintervall maximal 5 Ma. Dieses vorläufige Resultat ergibt eine Periode von weniger als 10 ka für die Latemar-Plattformzyklen, welche somit deutlich kürzer ist als die kürzeste Periode des Milankovitch-Spektrums.

Darüber hinaus dienen die Resultate einer präziseren Kalibration der bislang auf einer schwachen Datenbasis abgestützten triassischen Zeitskala. Das in verschiedenen aktuellen Zeit-

skalen angegebene Alter der Anis-Ladin-Grenze von 232–235 Ma beruht vorwiegend auf K–Ar- sowie ^{40}Ar-^{39}Ar-Analysen an Feldspäten vergleichbarer südalpiner Tuffite (HELLMANN und LIPPOLT, 1981) und müsste bei Berücksichtigung der im Rahmen dieser Studie ermittelten Resultate auf rund 240 Ma erhöht werden.

BRACK, P. und RIEBER, H. (1993): Towards a better definition of the Anisian/Ladinian boundary: New biostratigraphic data and correlations of boundary sections from the Southern Alps. Eclogae geol. Helv., 86, 415–527.

GOLDHAMMER, R.K., DUNN, P.A. und HARDIE, L.A. (1987): High frequency glacio-eustatic sea level oscillations with Milankovitch characterisctics recorded in Middle Triassic platform carbonates in northern Italy. Am. J. Sc., 287, 853–892.

HELLMANN, K.N. und LIPPOLT, H.J. (1981): Calibration of the Middle Triassic Time Scale by Conventional K–Ar and $^{40}Ar/^{39}Ar$ Dating of Alkali Feldspars. J. Geophys., 50, 73–88.

OBERLI, F., FISCHER, H. und MEIER, M. (1989): High-Resolution Zircon Dating of Tertiary Pyroclastic Sediments by Low-Level U–Pb Techniques. Abstr. 28th Int. Geol. Congress, Washington D.C., 2, 536–537.

Th. F. Nägler and R. Frei (Bern):

Initial and isotopic composition from ultramafic to acidic rocks of the Masirah ophiolite / Oman and their implications for Nd model age calculations.

Field- and sedimentary evidence within the Masirah ophiolite complex/Oman established generation of oceanic crust ≥ 140 Ma (faunal evidence; pers. comm. IMMENHAUSER, 1994) and the presence of two superposed nappes of oceanic crust (MARQUER et al., submitted). Most data discussed here are from the upper nappe. This upper nappe contains rocks which were formed during at least three different magmatic events: 1) generation of oceanic crust ≥ 140 Ma; 2) production of alkali magmatites and 3) emplacement of real K-feldspar granites.

ε_{Nd}[150 Ma] values of a variety of different rock types (i.e. troctolite, different gabbros, anorthosite, dolerite, pillow basalt, pegmatitic gabbro and granite) range from +7 to +9.7. Nd contents range from 0.16 (troctolite) to 64.5 ppm (pegmatitic gabbro). According to their Nd isotopic composition the rocks can be broadly subdivided into three different groups: I) rocks still showing Nd isotopic characteristics of depleted mantle (troctolite, gabbros, pillow basalt; $^{147}Sm/^{144}Nd \approx 0.2$), II) rocks with ε_{Nd}[0] values around +8 (pegmatitic gabbro, fine-grained gabbro, dolerite; $^{147}Sm/^{144}Nd \approx 0.17$) and III) acidic rocks with ε_{Nd}[0] values in the range of +5 to +6 (anorthosite, granite; $^{147}Sm/^{144}Nd \approx 0.08$). One gabbro (F-22) shows a relatively low ε_{Nd}[O] value of 6.55. Taking into account that published data from samples from Atlantic Mid Ocean Ridge basalts and basaltic glasses give a range of 6 ε_{Nd} units, the offset of F-22 can most easily be explained as a natural variation within oceanic crust. A continental crust contibution to this gabbro is not likely because of its tectonic position. Even if such a mixing is considered, the crustal component would have to be significantly smaller than 1% due to the very low Nd content of the gabbro (< 0.4 ppm).

U–Pb zircon data of a trachyte from the alkali volcanic suite give a magmatic age of 123 ± 2 Ma. One granite is significantly younger than 140 Ma (108 ± 1 Ma) and its Pb isotopic composition, corrected accordingly, also indicate a MORB-type source.

The tectonic setting of the acidic rocks and their initial Pb and Nd isotopic composition as well as the lack of correlation between Nd contents and isotopic composition exclude a significant admixture of continental material, although the sensitivity of the isotopic data towards such a contamination is large due to the extremely low Pb, U and REE concentrations (Pb: 0.008 ppm to 2.55; U: 0.002 ppm to 1.74; Nd: 0.16 ppm to 65 ppm). Taking the mean of massive gabbros and troctolite of the Masirah ophiolite as representatives of the upper mantle in terms of Nd and Pb isotopic composition and upper crust values from ZARTMAN and HAINES (1988) as representative of the contaminating continental crust a maximum contamination can be modeled. Only up to 12% (12%) of the Nd (Pb) present in the granite could be of continental origin. As the concentration of Nd (Pb) in the upper continental crust is more than 120 times (460 times) that of the Masirah ophiolite, the continental crust contribution to the generation of the granite must have been significantly below 0.2%. The initial isotopic signatures of the granite can however easily be explained without any crustal component, assuming granite derivation from a F-22 like mantle source. Thus, the present study reveals the likelihood of granite generation within the oceanic environment without addition of material from the continental crust.

Sensible Nd model ages can only be derived for rocks of group III ($^{147}Sm/^{144}Nd \approx 0.08$). Samples with $^{147}Sm/^{144}Nd$ ratios approaching ≈ 0.2 develop quasi parallel to the depleted mantle and thus there is no well defined intersection between sample- and mantle evolution line. As their source is devoid of old continental crust compo-

nents, the anorthosite and the granite should show Nd model ages (TDM) in the range of their magmatic age. However, even if the respective depleted mantle evolution model is based on the mafic samples from the same ophiolite, the difference between magmatic age and TDM is 40 Ma for the anorthosite and 160 Ma for the granite. The case of the anorthosite can be almost explained with analytical uncertainties alone, whereas the age discrepancy of the granite is clearly significant. Thus, natural variations in the Nd isotopic compositions of oceanic crust introduce another significant uncertainty to Nd model ages.

MARQUER, D., PETERS, T.J. and GNOS, E. (submitted): Re-interpretation of the Masirah ophiolite (Oman): No transform fault "Melange" but a Paleocene intraoceanic thrust.

ZARTMAN, R.E. and HAINES, S.M. (1988) The plumbotectonic model for Pb isotopic systems among major terrestrial reservoirs – A case for bi-directional transport. Geochim. Cosmochim. Acta 52, 1327–1339.

D. Nyfeler, Th. Armbruster, R. Dixon, V. Bermanec (Bern, Pretoria, Zagreb):

Nchwaningite, $Mn_2^{2+}SiO_3(OH)_2 \cdot H_2O$, a new pyroxene related chain silicate from the Nchwaning mine, Kalahari manganese field, South Africa.

Nchwaningite, $Mn_2^{2+}SiO_3(OH)_2 \cdot H_2O$ is an orthorhombic chain silicate (space group $Pca2_1$, Z = 4. a = 12.672(9)Å, b = 7.217(3)Å, c = 5.341(2)Å), occurring as pin cushion-like aggregates together with calcite, bultfonteinite and chlorite at Nchwaning mine, located in the Kalahari Manganese Field, Northern Cape Province, South Africa. The aggregates consist of light brown, transparent needles which average 1.0 · 0.1 · 0.05 mm in size. Nchwaningite is named after the mine Nchwaning II where it was found first. Nchwaningite is biaxially negative with the refractive indices $\alpha = 1.681(2)$, $\beta = 1.688(2)$, $\gamma = 1.690(2)$, $2V_x = 54.4°(4)$. The optical orientation is X = b, Y = a. Z = c. Nchwaningite has two perfect cleavages parallel to (010) and (100). The calculated density is 3.202 g/cm³. The chemical composition was determined by electron microprobe analyses, yielding minor substitutions of Mg for Mn.

The crystal structure including H positions was solved and refined from X-ray single-crystal data to R = 2.14, RW = 2.91. The nchwaningite structure consists of double layers of laterally linked so-called truncated pyroxene-building units formed by a double chain of octahedra, topped with a Zweier-single chain of Si tetrahedra. Symmetry equivalent units are linked laterally but turned upside down. This yields a double layer structure with hydrogen bridges linking the layers. A striking feature of the structure is the fact that one MnO_6 corner is formed by a H_2O molecule.

The tetrahedral chain and octahedral distortion of the new mineral is compared with pyroxenes having Mn^{2+} on M1 (synthetic $MnSiO_3$ ($P2_1/c$ clinopyroxene) and johannsenite $CaMn[SiO_3]_2$). To test a complete Ca and Mg substitution for Mn in the new nchwaningite structure type, distance least square refinements were performed. The generated structures were compared in terms of inter- and intrapolyhedral distortion. Based on differences from the cation valence and the calculated valence sums, an index expressing the distortion over the whole structure was calculated. By comparing all these data, there is no evidence that one of these structures is unlikely to be stable.

J.H. Partzsch und Ch. Meyre (Basel)

Die strukturelle Entwicklung der mittleren Adula-Decke (Zentralalpen, Schweiz).

Structural evolution of the middle Adula nappe (Central Alps, Switzerland).

Die durch eine eklogitfazielle Überprägung charakterisierte Adula-Decke, die sich östlich der Tessiner Kulmination befindet, nimmt innerhalb des penninischen Deckenstapels eine relativ tiefe tektonische Stellung ein. Von der Tambo-Decke im Hangenden ist die Adula-Decke durch die Misoxer Zone getrennt, von der Simano-Decke im Liegenden durch die Metasedimente der Soja-Mulde.

Dominiert wird die Adula-Decke von spätvariskischen ehemaligen Granitoiden (Phengit-Gneise und Augengneise) und älteren Metasedimenten (v.a. Metapelite). Eingeschaltet in das paläozoische Kristallin sind Bänder von Metabasiten (mit Eklogiten) und Mesozoikum ("internes" Mesozoikum). Diese Verschuppung von unterschiedlichsten Gesteinen deutet auf eine durchgreifende tektonische Zerschlitzung, die der eklogitfaziellen Überprägung vorausgeht ("Sorreda-Phase"; LÖW 1987). Markant sind die petrographischen Unterschiede zwischen dem hangenden und dem liegenden Teil der Adula: Im liegenden Teil, wo Eklogite bisher nicht nachgewiesen werden konnten, überwiegen Biotit-Gneise (im hangenden Teil Phengit-Gneise). Die

im hangenden Teil auftretenden Eklogite wurden während einer späteren temperaturbetonten Metamorphose überprägt. Im Untersuchungsgebiet reicht diese Überprägung bis in die Amphibolitfazies und ist in den meisten Lithologien umfassend, so dass Hochdruckparagenesen nur in einigen Eklogitboudins erhalten sind.

Zwischen hangendem und liegendem Teil der Adula-Decke können auch auffallende strukturelle Unterschiede festgestellt werden: Der basale Kontakt der Adula-Decke ist scharf begrenzt und von einem Mylonitgürtel begleitet, während im Gegensatz dazu im Hangenden eine intensive Verschuppung von Adula-Kristallin und Bündnerschiefern der Misoxer Zone zu beobachten ist. Strukturell werden die hangenden Partien der Adula-Decke durch die Deformationsstrukturen der D2-Phase ("Zapport-Phase"; Löw, 1987) geprägt: Eine penetrative Hauptschieferung liegt subparallel zu den Faltenachsenebenen von isoklinalen F2-Falten. Etwa N–S streichende Streckungslineare und eindeutige Schersinnindikatoren deuten auf einen nordwärts gerichteten Deckentransport während D2. Die nachfolgende Deformationsphase D3 ("Leis-Phase"; Löw 1987) verfaltet die Hauptschieferung und erzeugt nur lokal eine neue Schieferung (crenulation cleavage), die relativ steil nach SE einfällt. Die Faltenachsen der F3-Falten fallen nach ENE. Diese offenen D3-Falten werden gegen die Adula-Deckenbasis hin immer isoklinaler und drehen gleichzeitig in ein NW–SE-Streichen um. Parallel zu den Faltenachsenebenen der nun isoklinalen F3-Falten wird eine penetrative Hauptschieferung ausgebildet. Ein weiterer stufenloser Übergang führt in den Mylonitgürtel der Adula-Basis, der durch intrafoliale Falten charakterisiert ist. Damit ist der liegende Teil der Adula-Decke durch D3 geprägt (im Gegensatz zum hangenden Teil, der durch D2 geprägt ist). NW–SE streichende Streckungslineare und Schersinne, die eine Bewegung des Hangenden nach NW anzeigen, deuten darauf hin, dass die Adula-Decke während der Deformationsphase D3 auf die Simano-Decke überschoben wurde. Quarzstrukturen und synkinematisches Mineralwachstum (Czo + Pl + Hbl + Qtz) deuten auf metamorphe Bedingungen der untersten Amphibolitfazies (Ep-Amphibolitfazies).

Eindeutige Extensionsbewegungen konnten bisher nur innerhalb der Misoxer Zone nachgewisen werden, wo ein nach E fallendes Strekkungslinear und Scherbänder auf Bewegungen des Hangenden nach E unter grünschieferfaziellen Bedingungen (Quarzstrukturen, Chl auf Scherzonen) hindeuten. Diese Extensionsbewegungen sind auf die Aufdomung der Tessiner Kulmination zurückzuführen.

Löw, S. (1987): Die tektono-metamorphe Entwicklung der nördlichen Adula-Decke (Zentralalpen, Schweiz). Beitr. geol. Karte Schweiz NF 161.

Thomas Pettke, Larryn W. Diamond, Robert Frei and Igor M. Villa (Bern):

He, Ar, U–Pb and Rb–Sr isotope systematics of fluid inclusions in quartz, associated vein minerals and native gold from epigenetic late Alpine Au-veins in NW Italy.

He, Ar, U–Pb and Rb–Sr systematics have been investigated in epigenetic Au-quartz veins (Brusson, Monte Rosa district) on qtz (He, Ar, U–Pb, Rb–Sr), carbonates (carb: cal + dol; He, Ar, Rb–Sr), native Au (He, Ar, U–Pb), muscovites (Rb–Sr, ^{40}Ar-^{39}Ar) and bulk inclusion fluids extracted from qtz (Rb–Sr). The aim was to constrain the isotope evolution of these elements in the hydrothermal fluid at the site of mineral deposition in order to estimate characteristics of their respective sources and consequently to constrain possible sources of gold.

Rb–Sr results for Monte Rosa metagranite-hosted veins reveal a continuous decrease of the Sr initial ratio (Sr_{init}) with vein growth (from 0.729 to 0.714). Early qtz fluid inclusions cluster at 0.7245, those of late qtz at 0.7215, later carb have 0.714. Compared with Sr, ^{87}Rb/^{86}Sr ratios vary only slightly but also decrease with vein growth. The observed Rb–Sr evolution is attributed to decreasing fluid-wall rock interaction due to armouring of the unaltered host rock by vein mineralization and prograding alteration envelope. Metaophiolite-hosted thin veinlets crystallized from one single fluid pulse yield the lowest Sr_{init} = 0.708 and a Rb–Sr formation age of 30 Ma (qtz + cal + ms), confirmed by ^{40}Ar–^{39}Ar on ms.

Pb compositions of Fenilia vein qtz, py and native Au range between 17.45–19.45 (^{206}Pb/^{204}Pb), 15.46–15.76 (^{207}Pb/^{204}Pb) and 37.35–40.15 (^{208}Pb/^{204}Pb). U concentration, [U], is always low (< 350 ppb). In individual vein samples Pb in native Au is less radiogenic than all other minerals and is in Pb-isotope disequilibrium with both earlier qtz and the metagranite hostrock. [Pb] in native Au is highly variable (216–171370 ppb); low [Pb] correlates with a primitive Pb signature, high [Pb] with a radiogenic Pb signature. All Au samples show affinity with mantle Pb. Since native Au is late in the paragenetic sequence, and fluid-host rock interaction decreased with vein growth (see Rb–Sr results), the nonradiogenic source Pb-signature is partially preserved.

$^3He/^4He$ in all qtz and carb ranges between $3.5 \cdot 10^{-8}$ and $23.8 \cdot 10^{-8}$, higher than the mean crustal production ratio of $2 \cdot 10^{-8}$. This excess ^3He is interpreted as a small contribution of mantle He (~1%, see below). Consequently the mantle contribution in all other gases is insignificant. Metaophiolite-hosted thin veinlets have $^3He/^4He = 20.1 \cdot 10^{-8}$ to $23.8 \cdot 10^{-8}$. $^3He/^4He$ in > 1 m thick veins cutting various rock types all cluster between $8.4 \cdot 10^{-8} - 13.4 \cdot 10^{-8}$ (qtz) and $3.5 \cdot 10^{-8} - 6 \cdot 10^{-8}$ (carb) and show higher and variable Sr_{init} (0.7095–0.729). [He] varies up to three orders of magnitude, without affecting the He isotope ratios.

Two samples of free Au (~ 300 mg, Fenilia vein) were degassed in 5 steps. Most He was degassed below ~750 °C, presumably due to fluid inclusion decrepitation. The first sample gave $^3He/^4He = 34 + 9 \cdot 10^{-8}$, [4He] = 5.7 nl STP/g, the second $^3He/^4He = 28 \pm 10 \cdot 10^{-8}$, [4He] = 3 nl STP/g, $^{40}Ar/^{36}Ar \geq 5800 \pm 10$, $[^{36}Ar] < 15 \cdot 10^{-5}$ nl STP/g. These $^3He/^4He$ and $^{40}Ar/^{36}Ar$ ratios are significantly higher than in all qtz (0.084–0.107 and < 1450 respectively) from the same vein. Thus, He and Ar show isotope disequilibrium between native Au and coexisting vein minerals, in accordance with Pb results.

$^4He/^{40}Ar^*$ varies, even within individual veins, from 1.3 (veinlets in metaophiolite, late qtz from thick veins in metagranite) up to 23 (qtz from thick veins in metasediments and metagranite). The thicker the vein, the higher is the $^4He/^{40}Ar^*$. This variability indicates that the source of Ar differs from that of He, the former being dominated by the host rock. $^{40}Ar/^{36}Ar$ ranges between 500–2300 for qtz, and between 1530–2350 for associated carb. $^{40}Ar/^{36}Ar$ ratios below 1000 in qtz reveal an atmospheric Ar contribution. $^3He/^{36}Ar$ ratios of $\leq 10^{-4}$, however, are much higher than the atmospheric value of $23 \cdot 10^{-8}$, eliminating significant ^3He contribution from air and revealing high [He] in the fluid. The same is true for native Au ($^3He/^{36}Ar \geq 0.0056$).

Taking account of diffusive loss and radiogenic production affecting trapped gases, the bulk He–Ar signature for qtz + carb is interpreted to be the trapped signature. In 30 Ma, the low [U], [Th], [Li] and [K] in qtz + carb contribute less radiogenic ^4He, ^3He and ^{40}Ar than our analytical error. Furthermore, as retentivity for trapped He is higher than for radiogenic He associated with a recoil damage, in situ produced gases are more easily lost. If all $^4He^*$ produced from U/Th decay in 30 Ma was retained in the gold and assuming [Li] = 0, the trapped $^3H/^4He$ is calculated to be $= 60 \cdot 10^{-8}$.

Our results are consistent with metaophiolites being the ultimate source for most of the He, the nonradiogenic Pb component, some of the nonradiogenic Sr and hence probably most of the free gold. A metagranite source for free Au can be excluded (wrong Sr_{init} evolution with vein growth, less radiogenic He and Pb in free Au), a paragneiss source is in contradiction with the nonradiogenic Pb obtained on free gold. The broadly contemporaneous lamprophyres nearby can be excluded as a source for gold by means of the He signature.

He, Ar and Pb isotope disequilibrium between native Au and qtz + carb question the use of petrographically cogenetic vein minerals such as quartz to estimate processes responsible for Au deposition.

Th. Pettke, R. Frei and I.M. Villa (Bern):

U volatilization upon melting causes U–He age overestimates.

U–He dating of various minerals is presently experiencing a renaissance (e.g. WERNICKE and LIPPOLT, 1993, and refs therein), yielding apparently accurate formation ages. Dating of native Au, however, has yielded irreproducible ages mostly in excess of the known formation age, despite the apparently excellent He retentivity (NIEDERMANN et al., 1994). In these studies, attention has been focused on the $^4He^*$ retentivity of the samples investigated. Knowledge of other parameters such as the trapped He component (GRAHAM et al., 1987) and the U distribution within the sample are a prerequisite for the interpretation of the results. We therefore investigated the U concentration, [U], in various "aliquots" of 30 Ma native vein Au from Brusson (Monte Rosa Gold District, NW Italy), in both untreated and outgassed Au samples (molten, measured for He and Ar; PETTKE et al., 1994).

[U] measured by isotope dilution on native Au "aliquots" from the same hand specimens (Fenilia vein) yield scattered results by far exceeding analytical reproducibility, ranging from 12–351 ppb (n = 4) for hand specimen I and 3–47 ppb (n = 4) for hand specimen II respectively. [Pb] shows a similar variability, 216–171370 ppb in Au aliquots from hand specimen II. Our [U] results on Au compare with heterogeneous U distribution in hematite reported by WERNICKE and LIPPOLT (1993). Variable [U] in vein minerals such as native Au is interpreted to reflect that [U] in the fluid was not buffered during crystallization (i. e. no discrete U-phase such as pitchblende precipitated). Thus using "aliquots" of such samples for the determination of [U] required for

an U-He age and/or for the estimate of the trapped $^3He/^4He$ ratio (knowing $^3He^*$ from $^6Li(n, \alpha)^3H \rightarrow {}^3He$) yields inaccurate results. Therefore, the only viable procedure is to measure [U] on the same sample in which He was measured. Since Au has to be molten to extract rare gases, there is a danger of U volatilization upon melting, inducing U loss.

To examine this possibility, we loaded the native Au sample into a 30 cm long silica glass tube lining a furnace, and melted the Au at 1200 °C. This temperature, ~ 150 °C above the melting point of Au, is necessary to achieve quantitative outgassing of He. The silica tube was curved in such a way to ensure condensation of all compounds of interest. The bottom 10 cm of the furnace was directly surrounded by the heating coil. The low heat conductivity of quartz induces a considerable thermal gradient above the coil. After the He measurement, the silica tube was removed and the conspicuous, variably coloured condensates leached with dilute aqua regia, via a bottom leach and a tube leach (Fig. 1). The whole tube was leached again with concentrated aqua regia to test for the effectiveness of the dilute aqua regia leaches. The yield in the second total leach was only 0.1% of the total [U] and 3.4% of the total [Pb], showing that dilute aqua regia leaching was appropriate for U.

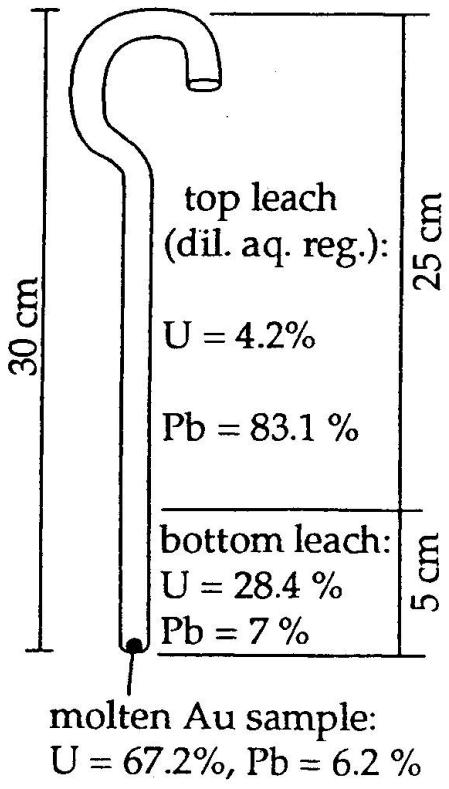

The results are given in figure 1. They demonstrate that $^1/_3$ of total [U] and more than $^9/_{10}$ of the [Pb] were lost from the Au upon melting. The accurate determination of [U] in an outgassed sample is only possible if the volatilized U is included in the calculations. As the percentage of U volatilization is probably a function of crucible temperature, it might be possible to get internally consistent, but too old, U–He ages by exactly repeating the outgassing procedure.

Conclusions

(1) Heterogeneous U distribution was found in Au: neither the true U–He age, nor the true trapped $^3He/^4He$ ratio can be determined using "aliquots".

(2) Melting for rare gas extraction results in U-loss by evaporation: parent element concentrations measured on the outgassed sample yield values, which are too low.

(3) Reproducibility alone does not guarantee accuracy.

GRAHAM, D.W., JENKINS, W.J., KURZ, M.D. and BATIZA, R. (1987): Helium isotope disequilibrium and geochronology of glassy submarine basalts. Nature, 326, 384–386.

NIEDERMANN, S., EUGSTER, O., THALMANN, C., FREI, R., KRAMERS, J.D., BRUNO, L. and HOFMANN, B. (1994): Trapped noble gasses in native gold; radiogenic He and fission Xe in U-rich minerals accompanying placer gold. Lunar and Planet. Sci., 25, 997–998.

PETTKE, TH., DIAMOND, L.W., FREI, R. and VILLA, I.M. (1994): He, Ar, U–Pb and Rb–Sr isotope systematics of fluid inclusions in quartz, associated vein minerals and native gold from epigenetic late Alpine Au-veins in NW Italy. Abstract (see this volume p. 310).

WERNICKE, R.S. and LIPPOLT, H.J. (1993): Botryoidal hematite from the Schwarzwald (Germany): heterogeneous uranium distributions and their bearing on the helium dating method. Earth Planet. Sci. Lett., 114, 287–300.

U. Poller, V. Liebetrau and Th. Nägler
(Fribourg, Bern):

Geochemical and isotopical investigations on S-type granitoids of the Silvretta crystalline complex.

The Silvretta crystalline complex, one of the upper Austroalpine nappes, bears beside amphibolites, gabbros, eclogites and paragneisses a large variety of orthogneisses. These are generally devided into two groups: the Flüelagranitic association and the so-called Older Orthogneisses including the Mönchalpgneiss.

Whereas the Mönchalpgneiss can be classified as metagranodiorite to metagranite, the Flüelagranitic Assoziation plots in the fields of monzo- to syenogranites. Using common discrimination diagrams an A-type character can be excluded for all samples. Main and trace element investigations applied on different classification models, assign S-type origin to the Mönchalpgneiss as well as to the Flüelagranitic association (CASTRO et al., 1991; HINE et al., 1978).

The original tectonic setting of the rocks was evaluated based on trace element plots (e.g. PEARCE et al., 1984). For most samples the within plate granites (WPG) and the ocean ridge granites (ORG) can be negated using Nb, Y and Si. Only a few orthogneisses of the Flüelagranitic association from one locality plot inside the WPG field because of exceptional high yttrium contents. Plotting Rb against Y+Nb the Mönchalpgneisses clearly occupy the volcanic arc (VAG) field, whereas the Flüelagranitic association plots in VAG and syncollision fields. REE patterns from all analyzed Silvretta gneiss types give a good conformity with VAG. All these results are describing the original tectonic environment of the pre-anatectic material.

Sm–Nd model ages from gneisses of both groups fall in a narrow range around 1.7 Ga. In contrast to these very homogeneous results of petrographical different rocks, the samples of the gneiss Urezzas (Flüelagranitic association) yields model ages between 1.2 and 1.5 Ga. However, a xenolith found in the Urezzas gneiss shows a model age around 1.6 Ga. These results are regarded as the reflection of mixing processes of at least 1.7 Ga old crust with various younger crustal components. This additional influence of juvenile crust is only present in parts of the Flüelagranitic association.

The developed model is supported by the reinterpretation of Rb–Sr isochron data of gabbroic and granodioritic rocks. The combination of this new interpretation with the mentioned Nd-model ages also bears information about the crystallization history of the different rocks.

CASTRO, A., MORENO-VENTAS, I. and DE LA ROSA, J.D. (1991): H-type (hybrid) granitoids: a proposed revision of the granite-type classification and nomenclature. Earth Sci. Rev., 31, 237–253.

HINE, R., WILLIAMS, J.S., CHAPPELL, B.W. and WHITE, A.J.R. (1978): Contrast between I- and S-type granitoids of the Kosciusko Batholith. J. Soc. Austr., 25, 219–234.

PEARCE, J.A., HARRIS, N.B.W. and TINDLE, A.G. (1984): Trace element discrimination diagrams for the tectonic interpretation of granitic rocks. J. of Petr., 5/4, 956–983.

D. Pozzorini (Zürich):

Tentative field calibration of oxygen isotope mineral pair geothermometers within a contact aureole. an example from the Ventina ophicarbonate zone, Valmalenco, Italy.

Contact metamorphism potentially provides steep temperature and metamorphic gradients that control mass exchange processes between the intrusion and the country rocks. Several studies have been performed with the purpose to quantify such exchange processes by use of stable isotope geochemistry (e.g. NABELEK et al., 1984, 1992). In these exchange processes, fluids are important transport media and in turn provide an excellent field of application for stable isotope geochemistry.

In most cases, the temperatures that characterize contact aureoles may be constrained by (1) the stability fields of the observed mineral assemblages represented in T-X_{fluid} space, (2) cation-exchange geothermometry and (3) oxygen isotope geothermometry.

Oxygen isotope fractionation factors between major rock-forming minerals for geothermometry purposes can be determined (1) experimentally, (2) theoretically and (3) by (semi-) empirical calibration of natural samples. For all three approaches, problems arise such as kinetic effects during exchange reactions especially at low temperatures for (1), incomplete sets of mineral-spectra (e.g. for water-bearing minerals) to apply statistical mechanical methods (2) and isotopic disequilibrium occurring in natural systems mostly due to retrograde exchange during fluid infiltration and/or diffusion processes for (3).

In the present work, oxygen isotope fractionations between calcite and antigorite have been determined and empirically calibrated with temperatures obtained by calcite-dolomite solvus thermometry and by other mineral-pair oxygen isotope thermometers in the geologically relevant temperature interval of 450–600 °C.

In the western part of the Malenco ultramafic body, a major zone of ophicarbonate rocks (Ventina ophicarbonate Zone, VOZ) is cut by the Bergell intrusion in the northwest and is exposed with a general steep NE-dip over a distance of about 6 km towards the southeast within and outside the Bergell contact aureole. The ophicarbonate rocks consist of a brecciated texture defined by schistose antigorite-serpentinite fragments of variable dimensions enbedded in a predominantly calcite matrix. Towards the intrusion, the ultramafic fragments become more massive due to antigorite break-down and growth of forsterite.

Oxygen isotope exchange mineral-pair thermometry (calcite-diopside and calcite-forsterite) of ophicarbonate rocks directly at the magmatic contact yields temperatures between 600 and 630 °C, distinctly higher than those obtained by calcite-dolomite solvus thermometry (550 °C, TROMMSDORFF and EVANS, 1977). In these rocks, retrograde antigorite is found growing on forsterite and be in textural equilibrium with chlorite and calcite. Oxygen isotope fractionations between calcite and retrograde antigorite (Δ = 2.8‰) are quite close to Δcalcitechlorite (= 2.6‰), supporting a very similar oxygen isotope fractionation of chlorite and antigorite with respect to calcite.

In the outer part of the contact aureole, temperatures obtained by calcite-dolomite thermometry within the ophicarbonates range between 450 and 500 °C (TROMMSDORFF and EVANS, 1977) and are concordant to the temperature estimates of Alpine regional metamorphism outside the contact aureole (400–450 °C, MELLINI et al., 1987). Oxygen isotope disequilibrium is clearly indicated by variations of Δcalcite-antigorite and/or Δcalcite-diopside in profiles across the VOZ, parallel to the contact metamorphic isograde. Thus, the calibration of Δcalcite-antigo-rite in this lower-temperature domain (450–500 °C) is difficult due to kinetic effects, fluid infiltration- and diffusion-processes.

MELLINI, M., TROMMSDORFF, V. and COMPAGNONI, R. (1987): Antigorite polysomatism: behaviour during progressive metamorphism. Contrib. Mineral. Petrol. 97, 147–155.

NABELEK, P.I., LABOTKA, T.C., O'NEIL, J.R. and PAPIKE, J.J. (1984): Contrasting fluid/rock interaction between the Notch Peak granitic intrusion and argillites and limestones in western Utah: evidence from stable isotopes and phase assemblages. Contrib. Mineral. Petrol. 86, 25–34.

NABELEK, P.I., LABOTKA, T.C. and RUSS-NABELEK, C. (1992): Stable isotope evidence for the role of diffusion infiltration and local structure on contact metamorphism of calc-silicate rocks at Notch Peak, Utah. J. Petrol., 33, 557–583.

TROMMSDORFF, V. and EVANS, B.W. (1977): Antigorite ophicarbonates: contact metamorphism in Val Malenco. Contrib. Mineral. Petrol. 62, 301–312.

C. Prospert and G.G. Biino (Fribourg):

Genetic mechanism of quartz-andalusite veins in the Silvretta nappe as suggested by field, microscopic and fluid inclusion data.

The occurrence of Qtz-And veins characterises amphibolite facies metasediments (metapelite, paragneiss and quartzite) of the Silvretta nappe (for a review, see MAGGETTI and FLISCH, 1993). In order to understand the formation of the veins and the related fluid circulation, a detailed structural investigation of a 4 km^2 area near Davos (Pischahorn) was carried out. The regional Variscan foliation Sv is oriented N120, 30–50° SW. The associated mineral (quartz, staurolite, micas) lineation Lv is intense and oriented E–W. Three generations of quartz veins have been distinguished.

The first type is void of andalusite and has been folded by the Variscan deformation responsible for Sv development. The second vein type contains andalusite. It parallels the foliation (Sv), and exhibits boudinage structures. Quartz stretching and andalusite orientation are parallel to Lv. These veins occur in "boudinage foliation" structures or are associated with brittle-ductile shear planes oriented N150–170, 50–80° SW-W. Shear criteria, parallel to the lineation E–W on the shear planes, indicate an apparent normal sense of movement to the W. The third vein quartz seldom contains andalusite. It is vertical and oriented N–S. These veins cross cut the foliation and the others veins.

In each type of vein, the internal microstructures of quartz shows both plastic deformation (evidence from subgrain formation or undulatory extinction) and grain boundary migration (often accompanied by "bulging"). Grain boundary migration and "bulging" have been interpreted as fluid phase activated recrystallization in grain boundaries rather than high temperature deformation. In the second vein type, quartz has smooth grain boundaries and is of homogeneous grain size. Moreover, quartz shows crystallographic preferred orientation. This observation has been interpreted as recrystallization under amphibolite facies. Formation of andalusite-quartz veins is clearly coeval with a deformation event (Late Variscan phase) which occurs after the Sv and extends from ductile to brittle microstructures.

Detailed microscopic observations and microthermometric analyses (using the USGS heating-freezing stage at CRPG-CNRS, Vandœuvre-lès-Nancy), were made on fluid inclusions in quartz from the second type of veins. Raman spectrometry data will be presented at the meeting. From cryometrie analyses, and according to the relative chronology, five main types of inclusions have been identified, but the earlier metamorphic fluids are mainly lost during plastic deformation and recrystallization.

Type (i) and (ii) are rare and isolated. Type (i) contains N_2 rich-fluid and the homogenization temperature (Th) ranges from –155 to –105 °C. Type (ii) is composed of salt water. The melting temperature (Tm) does not vary very much-be-

tween –20 and –25 °C. The most abundant fluid inclusions, types (iii), (iv) and (v), have been trapped in specific trails. Type (iii) has Th similar to (i) and is organized in long planes cross-cutting grains and subgrains. Types (iv) and (v) are aqueous fluid inclusions related to subhorizontal and subvertical small trails respectively. The Th ranges from –20 to –26 °C, as in type (ii) inclusions.

The abundance of N_2 rich fluid inclusions suggests that they must be related to an important fluid infiltration after vein formation during the late evolution of the Silvretta nappe.

MAGGETTI, M. and FLISCH, M. (1993): Evolution of the Silvretta Nappe. In VON RAUMER, J.F. and NEUBAUER, F. (eds): Pre-Mesozoic geology in the Alps. Springer-Verlag, 469–482.

F. Ried (Zürich):

Titanmobilität: Metasomatische Adern am Kontakt von Dolomitmarmoren zur Bergeller Intrusion.

Ti-mobility: metasomatic veins at the contact of dolomite marbles with the Bergell intrusion.

Titan gilt im allgemeinen als geochemisch immobil bei submagmatischen Temperaturen. Einige wenige Feldarbeiten belegen die Mobilität von Titan (z.B. GIERÉ, 1987; VAN BAALEN, 1994). In einem regelmässigen Adersystem am Kontakt von reinen Dolomitmarmoren zu Tonalit und Granodiorit der Bergeller Intrusion konnte die Mobilität von Titan nachgewiesen und quantifiziert werden. Die Mineralparagenesen erlaubten, die geologischen Rahmenbedingungen abzuschätzen. Mit Hydrothermalexperimenten unter den geologisch relevanten Bedingungen konnte die Löslichkeit von Rutil und die Art der Titankomplexe bestimmt werden.

Die metasomatischen Adern zeigen typischerweise eine symmetrische Anordnung der Mineralzonen: Dolomitmarmor // randliche Calcit-Olivin-Zone / zentrale Titanclinohumit-Spinell-(Calcit ± Dolomit ± Chlorit-)Zone. Die zentrale Zone wird sekundär in eine sulfidführende Phlogopit-Calcit-Zone umgewandelt.

Deformations- und Intersektionsbeziehungen belegen die mehrphasige Entstehung der Adern und erlauben, folgende Altersabfolge zu bestimmen:

1. Regionalmetamorphose mit Ausbildung der Hauptschieferung
2. Intrusion des Tonalits mit Bildung der Titanclinohumit-Spinell-Adern
3. Intrusion des Granodiorits mit Bildung der Titanclinohumit-Spinell-Adern
4. Intrusion von Pegmatitgängen und Ausbildung metasomatischer Kalksilikat-Adern (BUCHER-NURMINEN, 1981).

Die durch die Intrusion verursachten Alterationszonen am Kontakt von Intrusiva und Dolomitmarmor weisen keine direkte genetische Beziehung mit den Titanclinohumit- Spinell-Adern auf. Feldbeobachtungen belegen den genetischen Zusammenhang der Adern mit dem Bergeller Tonalit. Anreicherung von Uran und Thorium in metasomatischen Adern werden als Indiz für die Genese im Zusammenhang mit der Intrusion des Granodiorits betrachtet.

Die Entstehungsbedingungen der Adern sind T = 550 °C; P = ca. 3 kbar; $X_{CO_2} < 0.2$; $f_{HF} \approx 10^{-3.5}$; $fS_2 \approx 10^{-3}$. X_{CO_2} nimmt von den Dolomitmarmoren über die randliche Zone zur zentralen Titan-reichen Zone ab. Mit Massenbilanzrechnungen wurde die Zufuhr von Si, Ti, Al und Mg und die Wegfuhr von Ca beim metasomatischen Ersatz von Dolomitmarmor durch die Aderparagenese quantifiziert. Extrapoliert über einen detailliert kartierten Aufschluss von ca. 60 × 20 × 20 Metern wurde daraus eine Zufuhr von mehreren hundert Tonnen TiO_2 berechnet. Die abgeleitete TiO_2-Löslichkeit steht im Widerspruch mit bekannten, experimentell bestimmten TiO_2-Löslichkeiten in wässrigen Fluiden.

Aufgrund der Mineralzusammensetzungen und Paragenesen wurde geschlossen, dass Fluor die Löslichkeit von TiO_2 in wässrigen Fluiden erhöht. Löslichkeitsexperimente an Rutil in wässrigen Fluiden bei 550–650 °C, bei 3 kbar und mit unterschiedlicher HF-Konzentration demonstrieren die Abhängigkeit der Löslichkeit von der HF-Konzentration:

S_{TiO_2}, 550 °C = 0.00001 molal in wässriger Lösung

S_{TiO_2}, 550 °C = 0.00002 ... 0.016 molal in 0.1 ... 3.0 m HF.

Titan liegt dabei als $Ti(OH)_2F_2$-Komplex vor. Die experimentell ermittelten Löslichkeiten stimmen in der Grössenordnung mit den aus den Fluid/Gesteins-Verhältnissen und der Zusammensetzung der Adern berechneten Löslichkeiten überein.

BUCHER-NURMINEN, K. (1981): The formation of metasomatic reaction veins in the dolomitic marble roof pendants in the Bergell Intrusion (Province Sondrio), Northern Italy. Am. J. Sci, 281, 1197–1122.
GIERÉ, R. (1987): Quantification of element mobility at a tonalite/dolomite contact (Adamello Massif, Provincia di Trento), Italy, Diss. ETH Nr. 9141.
VAN BAALEN, M.R. (1994): Titanium mobility in metamorphic systems, a review. Chem. Geol., in press.

Paolo Scascighini (Fribourg):

Géologie et pétrologie de la Val Punt'Ota.

Geology and petrology of Val Punt'Ota (Grisons, Switzerland).

La Val Punt'Ota est une vallée nord-sud située à 7 km à l'ouest de Zernez (GR). Géologiquement elle se trouve dans la nappe cristalline de la Silvretta, dans l'unité de l'austro-alpin. Les principales roches qu'on y trouve ce sont des paragneiss (dépôt du protolite –1500 Ma), des métabasites à faciès éclogitique (cristallisation du protolite –1500 Ma), des vieux orthogneiss (cristallisation 895 Ma), des jeunes orthogneiss appartenant à l'association granitique de la Flüela (cristallisation 451 Ma) et des dykes tholéiitiques post-hercyniens.

Les éclogites ont constitué l'objet d'étude des dernières années et leur évolution a été reconstruite.

Le protolite basaltique cristallisé au précambrien (I) subit un métamorphisme amphibolitique avec hydratation (II) suivi d'un métamorphisme éclogitique avec déhydratation (III). Une remontée isotherme avec rehydratation (métamorphisme rétrograde) (IV–V) transforme les éclogites d'abord en éclogites symplectitiques et ensuite en amphibolites. La dernière phase métamorphique, à faciès schiste vert, est alpine (VI).

Sujet principal de mon étude est la caractérisation géochimique du passage éclogite-éclogite symplectitique-amphibolite enregistré dans les éclogites à grenat, les éclogites normales et les éclogites à zoisite.

MAGGETTI, M. et GALETTI, G. (1988): Evolution of the Silvretta eclogites: metamorphic and magmatic events. Schweiz. Mineral. Petrog. Mitt., 68, 467–484.

U. Schaltegger and F. Corfu (Zürich, Toronto):

U–Pb age determinations on rocks from the North Swiss Permo-Carboniferous trough and coeval basins of Central Europe: constraints for stratigraphy and late Variscan tectonics.

The final stages of continental collision during Variscan orogeny were characterized by dextral shear and extension or transtension. Starting in the Lower Carboniferous, extensional basins formed as a consequence of gravitative collapse of the overthickened crust. This was followed in the Upper Carboniferous by the development of Basin-and-Range tectonics related to lithospheric delamination. These extensional events formed a number of troughs such as the North Swiss Permo-Carboniferous Trough (NPT).

The NPT comprises 1000 meters of Westphalian, Stephanian and Autunian strata. The lower part of the sequence was deformed by a compressional event of unknown age (LAUBSCHER, 1987; DIEBOLD et al., 1992); the deformation is recognized by seismic studies, but not in the drill-cores.

U–Pb age determinations were carried out on detrital zircons from black siltstones and greywackes, and on volcanogenic zircons from two ash fall tuff layers from NAGRA drillcores of the Weiach well. The detrital zircons are derived from intrusive rocks in the adjacent basement areas and yield source ages mostly between 326 Ma and 332 Ma and possibly at 371 Ma , similar to intrusion ages of Black Forest granites. The youngest detrital zircons of 326 Ma define the maximum limit for the deposition of the lower part of the NPT.

The two tuff horizons at 1432 and 1586 meters depth were dated at 298 ± 1 Ma and at 303 ± 3 Ma, respectively. No volcanic strata could be detected below 1586 meters. The 298 Ma-old tuffs might originate from coeval explosive volcanic centers either in the Aar Massif or in the region of Northern Vosges – Saar-Nahe (BOUTIN et al., 1994; LIPPOLT and HESS, 1983). The age of 298 Ma is indicative for Upper Stephanian, which does not agree with the Autunian age deduced from the microflora. The Carboniferous/Permian boundary in the Weiach well, therefore, has to be located at a level higher than 1432 meters below surface.

Comparison with the Southern Vosges and the Aar massif: Volcanism and basin formation in the S' Vosges started earlier than 345 Ma and ended with explosive volcanism (subaerial ignimbrites) dated at 340 Ma. Thrusting along the "Ligne des Klippes" happened after 340 Ma and before granite intrusions at 336–339.5 Ma (K–Ar ages: MONTIGNY and THUIZAT, 1989; U–Pb ages: own data). Contemporaneous basin formation, magmatism and crustal anatexis argues for crustal thinning and high geothermal gradients already in Upper Visean to Namurian times. A coeval basin in the Aar massif (Bifertenfirn, Val Gliems) was deformed and overprinted by greenschist facies metamorphism before the intrusion of granites at 333 ± 2 Ma and of diorites at 310 ± 3 Ma (SCHALTEGGER and CORFU, 1995). Subsequent uplift caused the erosion of Westphalian strata between 310 and 300 Ma. Upper Stephanian short-lived basin formation, plutonism and explosive volcanism happened between 300 and 298 Ma, coeval with the higher-level Weiach tuffs.

The same period of tectonic instability may have been responsible for the uplift phase between 310 and 300 Ma in the Aar massif and the transtension in the lower part of the NPT. The widespread volcanic activity at ca. 300–298 Ma is an important stratigraphic marker in the Upper Stephanian of central Europe. It allows to date and correlate coeval volcanic or volcano-sedimentary strata in the Aar massif, Weiach and the Northern Vosges that have been stratigraphically classified in the Westphalian, Autunian and even Saxonian, respectively. The macro- and microflora, therefore, cannot be used as a stratigraphic marker, but is more likely indicative for paleoclimatic conditions.

The explosive volcanism at 300 to 298 Ma is calc-alkaline to sub-alkaline in composition and is typical for late-orogenic extension in an intracontinental setting. The geochemical characteristics are thought to be an inherited feature from the underlying crustal and mantle-derived sources. The zircons preserved inheritance of crustal components of Pan-African and Early Proterozoic age in both Namurian and Stephanian rhyolites.

This study demonstrates the paramount importance of precise U–Pb zircon dating for the understanding and regional intercorrelation of tectonic events during Late Variscan orogenic collapse.

BOUTIN, R., MONTIGNY, R. and THUIZAT, R. (1995): Chronologie K–Ar et $^{39}Ar/^{40}Ar$ du métamorphisme et du magmatisme des Vosges. Comparaison avec les massifs varisques avoisinants et détermination de l'âge de la limite Viséen inférieur – Viséen supérieur. Géologie de la France, in press.

DIEBOLD, P., NAEF, H. and AMMAN, M. (1992): Zur Tektonik der zentralen Nordschweiz. Geol. Ber. 14, Landeshydrol. u. -geol., Bern.

LAUBSCHER, H. (1987): Die tektonische Entwicklung der Nordschweiz. Eclogae geol. Helv. 80, 287–303.

LIPPOLT, H.J. and HESS, J.C. (1983): Isotopic evidence for stratigraphic position of the Saar-Nahe Rotliegend volcanism. I. $^{40}Ar/^{39}K$ and $^{40}Ar/^{39}Ar$ investigations. N. Jb. Geol. Paläont. Mh. 12, 713–730.

SCHALTEGGER, U. and CORFU, F. (1995): Late Variscan "Basin and Range" magmatism in the central Alps: Evidence from U–Pb geochronology. Geodin. Acta 8, in press.

S.A. Sergeev and R.H. Steiger (Zürich):

Caledonian and Variscan granitoids of the Gotthard massif: new geochronological and geochemical results.

The Gotthard massif is one of the tectonic windows in the Helvetic realm that offer insight into the pre-Permian crystalline basement of the central Alps. The symmetrical anticlinorium-like structure of the massif is dominated in its core by the 438 +5/–8 Ma old Caledonian orthogneiss (Streifengneis) representing Proterozoic units partly mobilized during the anatexis following the regional HPT metamorphism. During the Variscan tectonometamorphic cycle this same rock association was again subjected to partial melting which led to successive formation of the Variscan granitoids. The Variscan granitoids comprise 1) the partly isometric, gneissic granite-granodiorite stocks (Gamsboden, Fibbia, Medels, Cristallina), 296.0 ± 1.2 Ma old, exhibiting most of the S-type, collisional granitoid diagnostic features and 2) the massive more acidic granites (Rotondo, Tremola, Cacciola, Winterhorn, Mt. Prosa), 294.5 + 3.5/–2.0 Ma old, which are post-tectonic homogeneous granites of crustal origin, cropping out at the stock margins. The external zircons found in the Rotondo and Tremola granites imply an essentially Caledonian (~ 450 Ma old) protolith, whereas the Fibbia and Gamsboden gneissic granitoids were predominantly generated from two Proterozoic source rocks ≥ 740 and ~ 1760 Ma old. The Caledonian orthogneiss contains external zircon from only one Proterozoic source (~ 780 Ma old).

In spite of their contrasting structural and compositional setting, emplacement of all Gotthard Variscan granitoids occurred almost simultaneously. This paradox could be explained in terms of melt generation to various degrees of partial melting and by mobilization of divergent protoliths without mixing of the produced melts and with each of them rising to form a separate body. Such a mechanism does not call for source rocks much different from those of the para- and orthogneisses exposed as country rocks. The proportion of the pre-magmatic zircons decreases from several percent to a fraction of one percent with increasing intrusive and leucocratic affinities of the granitoids. In the Fibbia and Gamsboden bodies the inherited zircons of Late Proterozoic age and coeval zircons from a mafic xenolith show both isotopic readjustment at the time of the magmatic event. In contrast, the Early Proterozoic external zircons in the same granitoids were more intensively affected by post-magmatic metasomatism than by the magmatic melts. It may indicate different physical and/or chemical conditions of partial melting for the two sources and probably require a different degree of Zr saturation in the initial melts generated.

Geochemical features of all Variscan granitoids appear to be compatible with those of the Caledonian orthogneiss, a crust-derived granite. Rb vs Y+Nb and Y vs Nb diagrams show the

massive Variscan granites to be within-plate granites in origin. On the contrary, the gneissic granitoids and orthogneiss plot in the volcanic arc granite field. The REE abundance ΣREE = 119 ppm of the Variscan gneissic (vg) and 115 ppm of the Variscan massive (vm) granitoids and pattern [$(La/Yb)_N$ = 7.8 (vg) and 4.3 (vm)] are also similar to those of the Caledonian orthogneiss (co) ΣREE = 85 ppm, $(La/Yb)_N$ = 7.3]. This probably points to their origin from a related source as well as to similarity in the alteration processes. A strong correlation of Eu and Sr suggests that Eu/Eu* [= 0.4 (vg), 0.2 (vm) and 0.2 (co)] is controlled by Sr- and Eu-compatible phases, i.e. primarily plagioclase. Our petrographic observations suggest widespread metasomatic replacement of magmatic feldspar by microcline and albite. During this process most of the released Sr could be removed from the rock by fluids parallel with an increase in Rb. Isotope systematics of zircons separated from metasomatic microcline show post-magmatic disturbance which coincides with the Rb/Sr whole-rock age of 270 Ma for (vm), i.e. 25 Ma after the intrusive event. We consider the date of 270 Ma as the time of the petrographically advertised Si-alkali metasomatic event and microcline porphyroblastesis that propound reexamination of some Rb/Sr results, formerly interpreted as intrusive ages and still used as a datum for Variscan or Caledonian magmatic contributions in the Alpine foldbelt. The absence of Cadomian memory in zircon grains from all Gotthard granitoids derived from various crustal units implies an accidental role for Gondwana-incorporated material in this part of the European continental margin.

J. Spangenberg and L. Fontboté (Genève):

Rare earth element patterns in the host and gangue carbonates of the San Vicente zinc-lead deposit, Peru (see p. 271–275 in this issue).

J. Spangenberg, L. Fontboté, Z. Sharp and J. Hunziker (Genève, Lausanne):

Stable isotope (C, O) constraints on the mechanisms of ore precipitation in the Mississippi Valley-type Zn–Pb district of San Vicente, Central Peru. Evidence for fluid mixing, multiple fluid-rock interaction and CO_2-degassing.

The San Vicente Mississippi Valley-type (MVT) Zn–Pb deposit is hosted in carbonate rocks of the Pucara basin (Triassic-Jurassic) at the western margin of the Brazilian Shield, and is the major Zn-producer of Peru (14 Mt, 11% Zn, 0.8% Pb). The mineralization appears typically as a zebra ore, within alternating bands of dark replacement dolomite (DRD) and white sparry dolomite (WSD). The main ore-sulfide sphalerite occurs in the same paragenetic situation of the white dolomite: (I) as fine-crystalline anhedral sphalerite intergrown with white dolomite replacing the host DRD; (II) as coarse open space-filling subhedral sphalerite grown with WSD on altered DRD; (III) as a very coarse euhedral crystals within the late filling white dolomite, mainly as breccia-cement.

The carbon and oxygen isotopic composition of the altered host and gangue carbonates and associated organic matter show a strong regional homogeneity, suggesting that the physicochemical conditions and the fluid-rock interaction mechanism were uniform and almost constant during ore and gangue precipitation in the whole district.

Quantitative modeling of the $\delta^{13}C$ vs $\delta^{18}O$ covariations in the different carbonate generations provides new insights on the fluid(s) chemistry and the ore-forming processes. The models were computed using 1) mass balance equations for fluid mixing and water-rock interaction (ZHENG and HOEFS, 1993), and 2) Rayleigh distillation equations (ZHENG, 1990) for precipitation of carbonates during CO_2-degassing. The precipitation

Gangue mineral	$\delta^{13}C$ ranges (‰ PDB)	$\delta^{18}O$ ranges (‰ PDB)
Dark replacement dolomite, DRD (38)	0.5 to 2.5	–9.8 to –6.3
White sparry dolomite, WSD (158)	–0.1 to 1.7	–11.8 to –7.3
Late filling dolomite (10)	–0.3 to 1.1	–12.5 to –9.8
Late filling calcite (25)–11.5 to 0.7	–11.5 to 0.7	–15.1 to –9.8
Dolomite replacing evaporitic gypsum (7)	–0.4 to 1.0	–12.1 to–9.8
Calcite replacing evaporitic gypsum (11)	–4.5 to 0.8	–16.1 to–9.5
Organic matter associated to DRD (3)	–27.0 to –26.8	
Hydrothermal bitumen (9)	–27.5 to –23.0	

of the syn- and post-ore carbonate generations involve mixing of the native formational fluid (e.g. parent fluid of the unaltered host dolomite) with a hot slightly acidic incoming fluid. The ore forming solution can be considered as a thermally and compositional evolved meteoric ground water, whose chemistry was controlled during the transport by multiple and prolonged fluid-rock and fluid-fluid mixing. The measured isotopic variation of the ore-stage dolomites matches models of fluid-rock interaction in terms of 1) isotopic alteration of the host dolomite by the incoming ore fluid and precipitation of white dolomite and sphalerite I and 2) precipitation of dolomite and sphalerite II from the ore fluid, that evolves during exchange with the host dolomite. The isotopic composition of the late filling white dolomite (or calcite) associated to the sphalerite III is quantitatively modeled by CO_2-degassing and cooling of the ore fluid. Therefore, pressure variability plays a major role in the ore precipitation during the late hydrothermal events in San Vicente. These results suggest that the mineralizing processes were similar in the whole ore-district, and support the existence of a regional mineralizing hydrothermal system with interconnected plumbing.

This study is supported by the Swiss National Science Foundation (Grant No. 20.36397.92) and is a contribution to IGCP project n° 342 (Age and Isotopes of South American Ores). We are grateful to San Ignacio de Morococha S.A. Mining Company and the staff of the Geology Department of San Vicente mine for their help in the field work.

ZHENG, Y.-F. (1990): Carbon-oxygen isotopic covariation in hydrothermal calcite during degassing of CO_2: a quantitative evaluation and application to the Kushikino gold mining area in Japan. Mineralium Deposita, 25, 246–250.

ZHENG, Y.-F. and HOEFS, J. (1993): Carbon and oxygen isotopic covariations in hydrothermal calcites. Theoretical modeling on mixing processes and application to Pb–Zn deposits in the Harz Mountains, Germany. Mineralium Deposita, 28, 79–89.

J. Stolz, M. Engi and Mathias Rickli (Bern):

Tectonometamorphic evolution of SE Tinos, Cyclades, Greece.

The main tectonic unit making up Tinos island consists of continental margin rocks (volcanodetrital schist, minor marble). These rocks underwent Eocene subduction with metamorphism at > 40 km depth, prior to pervasive, fluid-driven retrogression associated with emplacement into higher crustal levels. Locally this lower unit *(LU)* is overlain by an ophiolite unit – serpentinized harzburgite metagabbro, greenschist ophicarbonate – lacking high pressure relics. In southeastern Tinos detailed investigation of amphibole zoning indicates that the earliest metamorphic relics of the upper unit *(UU)* are of low-pressure greenschist facies and may be oceanic. The tectonic contact between the two units, interpreted to represent a low-angle normal fault by AVIGAD and GARFUNKEL (1989) remains difficult to interpret kinematically on the basis of field data. However, the subsequent evolution of the two tectonic units, including a regional medium-pressure greenschist facies event, appears to have been very similar. Their mesoscopic structural characteristics (coaxial folds, parallel axial planar schistosities) are identical. Together these findings indicate that the two units acted as a coherent stack during the subsequent thrusting event that emplaced them on top of the virtually unmetamorphosed sediments exposed in the Panormos window of northern Tinos. The timing of this emplacement remains unclear but it is likely to predate the intrusion (at a depth of 7 ± 2 km) of Miocene granites in southern Tinos. Their contact aureole affects both the lower and upper unit rocks. During the final stages of uplift the contact at the base of the upper unit was reactivated displacing the hangingwall to the N by some 500 m.

Greenschists of the *LU* and the *UU* are very similar in their petrography. In the contact zone between the two units, mylonitic types prevail, and the precise location of the tectonic boundary is often difficult to map. Geochemical data provide a means to distinguish greenschists of the LU from those of the UU. Furthermore these data point to a range of source materials for the UU metabasic rocks: Beside the common MORB-affinity more evolved ferro-gabbroid dykes occur, and a minor gabbro suite with boninitic (?) character was found. The significance of these is presently not understood.

AVIGAD, D. and GARFUNKEL, Z. (1989): Low-angle faults above and below a blueschist belt – Tinos Island, Cyclades. Terra Nova 1, 182–187.

C.S. Todd, M. Engi, D.R. Schmatz (Bern):

Meso-Alpine conditions of regional metamorphism: thermobarometric data from Penninic rocks between Bellinzona and Brig.

The Lepontine dome in the central Alps exposes amphibolite grade metamorphic rocks of meso-Alpine (mid-Tertiary) age over an area

~ 100 × 50 km. In addition to a well established pattern of metamorphic isograds, individual pressure and temperature estimates by various authors exist in the literature. However, a coherent P-T-interpretation has been hindered due to the use of different calibrations of thermometers and barometers.

Where published mineral compositions allowed, we calculated P & T of meso-Alpine parageneses using a consistent thermodynamic database and mineral solution models. New samples were collected from the field where the geographic spread of samples from the literature was inadequate (new data chiefly from post-hercynian samples of the Simplon pass area, Val Antigorio and Valle Maggia). Mapped isograds in the Lepontine region provide additional constraints on pressure and temperature.

From this information, P & T were fit as a function of horizontal position and elevation. We used these metamorphic field gradients to assess the petrological significance of isograds from the area (Sta-in and Sil-in for pelites, Tr+Cal-in and Di+Cal-in for carbonates). Results indicate that pressure at the Sta-in isograd was around 6 kbar. The highest grade portions of the area reached just over 700 °C and 8 kbar, but the regional maxima in P & T do not coincide. The thermobarometric patterns supplement recent tectonic models of the central Alps based on seismic profiles. Together, these further constrain kinematic models of the meso-Alpine orogeny and subsequent uplift history.

P. Ulmer, E. Guggenbühl, V. Trommsdorff and A.B. Thompson (Zürich):

Stability of antigorite to 80 kbar: a potential source of H_2O in deep subducted oceanic lithosphere.

The high pressure stability of antigorite is fundamental for the understanding of H_2O storage and recycling during subduction of oceanic lithosphere. Antigorite contains approximately 13 wt% H_2O (28 mol%) and often constitutes 90% of hydrated peridotites. Natural examples of ultramafic complexes subjected to eclogite-facies metamorphism (Zermatt-Zone Switzerland; Erro-Tobbio Liguria Italy) indicate that antigorite is stable in excess of 600 °C and 25 kbar.

Previous high pressure experimental studies on the stability of serpentine have been performed with two different starting materials: KITAHARA et al. (1966) and YAMAMOTO and AKIMOTO (1977) used synthetic starting materials in the system $MgO–SiO_2–H_2O$ (MSH) which resulted a very limited high pressure stability of serpentine (< 550 °C at 10–50 kbar) but large stability fields of hydro-magnesium-silicate phases A and D were encountered at high pressures (≥ 30 kbar). EVANS et al. (1976) performed experiments with natural antigorite up to 15 kbar. They observed a much higher temperature stability for antigorite (660 °C at 15 kbar). This apparent discrepancy can most probably be attributed to the difference in starting material. Calculations using internally consistent data bases result in notable backbending of the equilibrium tc + fo = 5 en + H_2O and intersection with the equilibrium ant = 18 fo + 4 tc + 27 H_2O at 16 kbar.

In the present study *a natural, well characterized antigorite* (MELLINI et al., 1987) from a serpentinite of the Malenco ultramafic unit was used as starting material. The separated sample consists of 80% antigorite and 20% brucite. The starting mixture was made from 90% of the separate and 10% high temperature products (forsterite – enstatite) obtained by reacting the original material at 10 kbar 900 °C for 48 hours. This arrangement is similar to the one used by EVANS et al. (1976). H_2O saturation was achieved through the presence of brucite which reacts at low temperatures with antigorite to form forsterite and H_2O.

Experiments up to 35 kbar were performed in a piston cylinder apparatus using NaCl assemblies. The samples were encapsulated in 2.3 mm $Ag_{75}Pd_{25}$-containers and welded shut. Experiments from 35 to 80 kbar were performed in a Wacker-type multi-anvil apparatus. The starting material was contained in 1.6 mm OD Pt or $Ag_{50}Pd_{50}$ capsules. Run duration varied from 40 hours at high pressures to 120 hours at 15 kbar. The recovered charges were analysed by powder X-ray diffraction and electron microprobe.

Antigorite is stable to at least 70 kbar; at 77 kbar and 500 °C no antigorite was found, but norbergite ($Mg_3SiO_4(OH)_2$), overgrown (quench from fluid) by an unknown phase with the composition $Mg_4Si_3O_9(OH)_2$ was observed. Above 54 kbar a 10-Å-phase ($Mg_3Si_4O_{10} \cdot 2\ H_2O$, metastable quench?) was observed. The reaction ant = 18 fo + 4 tc + 27 H_2O has a positive slope, consistent with the results of EVANS et al. (1976) and terminates at an invariant point (in the MSH system) at 22 kbar and 710 °C, instead of 640 °C/16 kbar in the calculated phase diagrams. The reaction ant = 14 fo + 20 enstatite + 31 H_2O has a negative PT-slope. Refinement of thermodynamic data from the experiments is, however, inappropriate at the present state of knowledge.

The experimental results presented above show that antigorite is a stable phase in peridotite bulk compositions at low temperatures to at least 62 kbar (200 km). Antigorite breaks down to forsterite + talc + H_2O at pressures less than 22 kbar. At higher pressures antigorite breaks down directly to the hydrate free assemblage forsterite + enstatite + H_2O. This implies that the release of H_2O from deeply subducted serpentinized peridotites could be either stepwise (in "hot subduction environment"; slow subduction, young oceanic lithosphere) with intermediate talc, or single step ("cold subduction; fast subduction old oceanic lithosphere). Thus there is a considerable potential of antigorite to store and transport H_2O deeply into the upper mantle, where its breakdown can lead to mantle metasomatism and generation of arc-type magmas in the overlying mantle wedge.

EVANS, B.E., JOHANNES, W., OTERDOOM, H. and TROMMSDORFF, V. (1976): Stability of chrysotile and antigorite in the serpentine multisystem. Schweiz. Mineral. Petrogr. Mitt., 56, 79–93.

KITAHARA, S., TAKENOUCHI, S., and KENNEDY, G.C. (1966): Phase relations in the system $MgO–SiO_2–H_2O$ at high temperatures and pressures. Am. J. Sci., 264, 223–233.

MELLINI, M., TROMMSDORFF, V. and COMPAGNONI, R. (1987): Antigorite polysomatism: behaviour during progressive metamorphism. Contrib. Mineral. Petrol., 97, 147–155.

YAMAMOTO, K. and AKIMOTO, S.-I. (1977): The system $MgO–SiO_2–H_2O$ at high pressures and temperatures stabllity field for hydroxyl-chondrodite, hydroxyl-clinohumite and 10 Å phase. Am. J. Sci., 277, 288.

I.M. Villa, J.H.R. Eikenberg, E. Lehmann
(Bern, Villigen):

Zircon kryptoxenology.

Xe_f–Xe_n dating by neutron irradiation was established 20 years ago (SHUKOLYUKOV et al., 1974). Xe_f from spontaneous fission can be discriminated from reactor-produced Xe_n owing to the different isotopic composition reflecting different fission yields. Our modification includes Kr and the use of short-lived ^{85}Kr and ^{133}Xe to constrain Kr_n and Xe_n. Our procedure is:

1. Separation of ≈ 95% pure zircons. While U/Pb always requires handpicking to eliminate possible Pb-rich phases, U–Kr–Xe only needs to avoid secondary U minerals.

2. Computer simulation, via cross-sections, of *all* induced activities as a function of fluence and cool-off time; we were interested both in short-lived U-proxies (^{239}Np, $^{133-135}Xe$,...) and in potential health hazards (such as $^{132}Te/I$, $^{140}Ba/La$...).

3. Thermal neutron irradiation of unknown samples together with age monitors.

4. Hot-lab γ spectroscopy of ^{239}Np to calculate U (as well as further trace elements from other radioisotopes) .

5. Cooling period minimizing health hazards but limiting ^{133}Xe decay.

6. Stepwise heating analysis of Kr and Xe with a MAP 215–50™ rare gas mass spectrometer.

Results: We established the feasibility on magmatic zircons from the Limpopo belt, Zimbabwe, whose concordant U/Pb age is 2591 ± 1 Ma. We observed:

a) The measured activities match the calculations to better than 10%, except for a 70% ^{135}Xe depletion; ^{135}Xe is a well-known thermal neutron absorber and produces (excess) ^{136}Xe. The U content determined from Np agrees with U/Pb mass spectrometry. This is a second important procedural check.

b) The finite half-life of precursor nuclides $^{131-2}$(Te, I) and the ^{135}Xe interference on ^{136}Xe can be reasonably well corrected for. We determined a half-life of 4.8 d (instead of 5.2) for ^{133}Xe, basing on four $^{133}Xe/^{134}Xe$ measurements spanning 40 days (≈ 8 half-lives). With this correction, the calculation of Xe_n from ^{133}Xe is more precise than the partition into Xe_f and Xe_n basing on the small differences in endmember compositions (SHUKOLYUKOV et al., 1974).

c) The age spectrum shows a staircase shape despite the zircon being geologically undisturbed. This is an artefact caused by Xe_n reimplantation during irradiation of pure zircon, while some naturally-produced Xe_f recoiled out into the minerals surrounding the zircon in the granite.

d) If in-vacuo degassing was Fickian, then the ratio of artificial isotopes, $^{85}Kr/^{133}Xe$, should follow Rayleigh fractionation, as both derive from the same target, U, but it jumps irregularly. This reinforces EIKENBERG's (1988) observation that in 14 unirradiated overprinted U-minerals the elemental fractionation $^{86}Kr/^{136}Xe$ is compatible with volume diffusion in only one case.

Conclusions: What are the main advantages of the $^{85}Kr/^{133}Xe$ technique?

1. Complementarity to U/Pb, possible screening of most suited samples for handpicking.

2. Potential to date minerals where U/Pb dating is hampered by common Pb.

3. Usual advantage of stopwise heating: constraining formation ages despite disturbances.

4. Filtering non-ideal variations of Kr/Xe fractionation during stepwise heating by examining $(^{86}Kr_f/^{136}Xe_f) / (^{85}Kr/^{133}Xe)$.

5. Assessment of kinetic processes: using two noble gases is one step further than $^{40}Ar/^{39}Ar$, be-

cause it allows to document non-fickian transport simply by comparing element ratios while such a proof in the latter case is much more elaborate.

EIKENBERG, J.H.R. (1988): Vergleichende Datierung von Uranmineralien mit den U–Xe, U–Kr und U–Pb Systemen sowie Untersuchungen der Produktion von Ne und Ar durch Kernprozesse. Ph. D. Thesis Nr. 8522, ETH Zürich, 202 pp.

SHUKOLYUKOV, Y.A., ASHKINADZE, G.S., KOMAROV, A.N. (1974): Novyi neitronno-induktsionnii Xe–Xe metod mineral'noi geokhronometrii. Dokl. Akad. Nauk SSSR, 219, 952–954.

R. Wyder, M. Frey, L. Hauber and S. Schmid (Basel):

Die Kakirite des Tavetscher Zwischenmassivs aus den Neat-Sondierbohrungen 1991–1993.

Kakirites of the Tavetsch massif from NEAT drill holes.

Im Zuge des NEAT-Vorprojektes wurden in den Jahren 1991 bis 1993 im Tavetscher Zwischenmassiv drei Schrägbohrungen mit einer Gesamtlänge von 2156.80 m (SB-1 Nord: 833.50 m, SB-2 Süd: 543.30 m, SB-3 Tujetsch: 780.00 m) abgeteuft. In die Horizontale projiziert, entspricht dies einer Distanz von ca. 1550 m.

Die Bohrungen erbrachten zwei sehr wichtige Resultate: Die Nordgrenze des Tavetscher Zwischenmassivs wird im Raum Sedrun nicht durch mesozoische Sedimente der Disentiser Zone gebildet, sondern durch einen mit Clavaniev-Zone bezeichneten Bereich, der hauptsächlich aus zwei kakiritischen Hauptstörungen mit vielen Nebenstörungen gebildet wird. Die nördliche kakiritische Hauptstörung, mit etwa 20 m Mächtigkeit, enthält Gesteine des Aarmassivs wie auch des Tavetscher Zwischenmassivs und bildet somit die nördliche Grenzzone des Tavetscher Zwischenmassivs zum Aarmassiv (SCHNEIDER, 1992). Der zweite Befund ist die Tatsache, dass die gesamte erbohrte Strecke von mehr oder minder mächtigen Kakiritzonen gestört ist. Während in den Bohrungen SB-1 Nord und SB-2 Süd keine statistischen Angaben über die Häufigkeit der Kakiritzonen erhältlich sind, konnte der Kakiritanteil in SB-3 Tujetsch durch hohen Kerngewinn (Kernverlust < 3,50%) und eine akkurate Statistik auf 30% (bezogen auf die Bohrlänge) festgesetzt werden. Dabei wurden auf der Bohrstelle diejenigen Gesteine als Kakirite angesprochen, welche ohne mechanische Hilfsmittel von Hand desaggregiert und zerstört werden konnten. Die restlichen 70% der erbohrten Gesteine müssen als sehr mürbe, bis in seltenen Fällen hart und fest, bezeichnet werden.

Zwei mesoskopisch unterscheidbare Typen von Kakiriten wurden zutage gefördert. Den Hauptanteil in SB-3 Tujetsch bilden kakiritisierte Schiefer, seltener Phyllite und Gneise, welche noch das ursprüngliche, alpin gebildete Gefüge zeigen, jedoch keine Festigkeit und Kohäsion mehr besitzen. Der Kohäsionsverlust tritt vor allem entlang der Hauptschieferung als verlehmte S-Flächen auf. In vollständig kakiritisierten Bereichen ist praktisch jede Hauptschieferungsfläche von einem lehmigen Film, einem grauen, sandig-tonigen Brei noch unbekannter Zusammensetzung, belegt. Zusätzlich werden die Gesteine von lehmigen, subparallel bis senkrecht zur Hauptschieferung verlaufenden Klüften durchsetzt, so dass im Extremfall das Gestein aus einem sehr dichten Netzwerk aus lehmigen Klüften besteht und damit jede Kohäsion verliert. Die Übergänge von nicht kakiritisierten zu kakiritisierten Zonen äussern sich als eine innerhalb sehr kurzer Distanz (< 1 m) auftretende Zunahme der Klufthäufigkeit. Die Mächtigkeiten dieser Zonen in SB-3 Tujetsch betragen zwischen einigen Zehner Zentimetern bis maximal 50 m.

Der zweite Typ Kakirit repräsentiert die vollständige Zerstörung des alpinen Gefüges durch Scherbewegungen entlang schmaler Zonen. Dabei werden Gesteinskompartimente und einzelne Mineralien im mm- bis cm-Bereich aus dem Gefügeverband gerissen, abradiert, gerollt und zerbrochen. Diese "Zermahlung" des Gesteins führt zu einer dramatischen Korngrössenreduktion. Das Endprodukt bildet eine kohäsionslose, submikroskopisch feinkörnige Matrix (engl.: "gouge"), in der eckige Mineral- und/oder Gesteinssplitter schwimmen (kataklastische Textur). Dieser Typ Kakirit tritt nur in diskreten und schmalen Zonen auf. In SB-3 Tujetsch betragen die Mächtigkeiten solcher Zonen zwischen einigen Zentimetern bis maximal 1,20 m. Im nördlichen Bereich des Tavetscher Zwischenmassivs nimmt die Häufigkeit und Mächtigkeit dieser Kakirite zu. Besonders spektakuläre Beispiele wurden im Bereich der Clavaniev-Zone erbohrt.

Strukturell stellen die Kakirite des zweiten Typs die jüngste Deformationsphase des Tavetscher Zwischenmassivs dar. Sie durchschlagen jede andere Struktur, auch Kakiritzonen des ersten Typs. Während Kakirite des ersten Typs meist subparallel bis parallel zur Hauptschieferung verlaufen, sind Kakirite des zweiten Typs sehr häufig diskordant ausgebildet. Möglicher-

weise ist die Kakiritisierung der Gesteine ein Prozess, der noch rezent aktiv ist.

Hand in Hand mit der Kakiritisierung geht eine Mineralneubildung einher. Durch die Wechselwirkung von zerriebenem Gestein mit (evtl. meteorischem?) Wasser bilden sich neue Schichtsilikate. Von besonderem Interesse ist dabei die Bildung von Tonmineralien, insbesondere quellbarer Varietäten. Der Zusammenhang zwischen Kakirittyp, Ausgangsgestein und neugebildeten Mineralien muss noch eruiert werden.

SCHNEIDER, T.R. (1992): Gotthard Basistunnel. Auswertung der Sondierungen Tujetsch 1991. Bericht Nr. 425ah.

Roger Zurbriggen (Bern):

The Strona-Ceneri zone: a Variscan metamorphic core complex? Implications for the southern Alps.

The formation of the schlingen (due to F3-folding of the "main schistosity" S2 of the Ordovician metagranitoids) was accompanied by prograde amphibolite facies metamorphism and may represent the main Variscan event (ZURBRIGGEN, 1994). If so, two questions arise: (1) How old is S2? (2) What are the kinematics of the schlingen?

Evidence pointing to Ordovician/Silurian syn- and subsequent post-magmatic age of S2 include: D2 structures are geometrically identical to pre-metagranitoid D1 structures. Both are mylonitic and may represent a continuous deformation event during which the Ordovician granitoids intruded. This syntectonic interpretation would account for the homogeneous foliation (S2), and high aspect ratios (up to 1 : 40) of the plutons their essentially concordant intrusive contacts and it would provide a solution to the emplacement problem of these granitoids (orthogneisses"). Incompetently F2-folded leucosomes of coeval migmatites point to simultaneous tectonics. The latter have mobilized the large amounts of anatectic magmas that form the Ceneri gneiss bodies. These occur in a SW–NE oriented zone and probably represent a syn-migmatic suture that triggered surge tectonics (HOLLISTER and CRAWFORD, 1986). I correlate the "main schistosity" event D2 with the synmagmatic "main metamorphic" event (Ordovician/Silurian lower intercept U–Pb ages of PIDGEON et al., 1970). These nearly identical ages for metamorphism and magmatism support a syntectonic interpretation of the metagranitoids too. 370 Ma was widely interpreted to be the age of the "main deformation" D2 (FLISCH, 1987), but this seems less probable in the light of recent sedimentological data for the Austro- and Southern Alpine domains which indicate extensional tectonics for this period (LOESCHKE and HEINISCH, 1993; NEUBAUER and SASSI, 1993). The high thermal gradient in that rifting phase probably influenced the isotopic systems and weakened the crust.

Especially that weakness, the preexisting steep planar fabrics (S0, S1 and S2, ZURBRIGGEN, 1994) and their orientation subparallel to the shortening direction of D3 were responsible for the formation of the schlingen at mid-crustal amphibolite facies levels. Simultaneous nappe tectonics thickened the uppermost crust. This compressive phase D3 ended prior to 325 Ma, at which point mica cooling ages indicate decreasing metamorphic conditions (MCDOWELL, 1970). The resulting overthickened crustal welt became unstable as soon as compressive forces decreased or changed direction. SCHUMACHER (1994) and HUISMANS (1994) described the Val Colla line (VCL; D4) as a late Variscan, subhorizontal, > 1 km thick mylonite zone. Acting as a detachment fault, it may have brought up the amphibolite facies schlingen of the "*Strona-Ceneri core complex*" next to the Variscan greenschist facies rocks of the Val Colla zone. Extensive erosion of a rough surface is represented by the syntectonic Westphalian B/C (JONGMANS, 1960) conglomerates in graben structures.

There are striking analogies to the Cordilleran extensional tectonics (CONEY, 1987), where a first phase of extension brought up the metamorphic core complexes, and a second phase of extension (Basin and Range type) was associated with strike slip tectonics. The Southern-Alpine Permian magmatism (parts of the Ivrea mafic complex, Brissago dyke swarm, Baveno granite suite and Lugano volcanics) is coeval with this second transtensional phase (D5) during which the Cossato-Mergozzo-Brissago line (CMBL; BORIANI et al., 1990) was important, decoupling the Strona-Ceneri zone and the uprising Ivrea zone (IZ). Magmatic underplating of the mafic complex and large oblique slip tectonics (dip-slip and sinistral strike-slip components) along the CMBL may have produced steep planars in the SE of the IZ, at the same time as flat-lying planars were formed in the NW of the IZ. The early Mesozoic Pogallo line (D6; HANDY, 1987) is mainly a reactivation of parts of the CMBL. Both are very similar in kinematics. Alpine transpression (D7) folded the subhorizontal planar structures in the NW–IZ under greenschist facies conditions, forming the Proman antiform.

Conclusions

1) There are two phases of post-D3, late Variscan extension: D4 (~ 325–295 Ma): uplift of the "*Strona-Ceneri core complex*" along the "Val Colla low angle detachment fault" (VCL); and D5 (~ 295–260 Ma): synmagmatic uplift of the IZ along the CMBL.

2) Southern Alpine basement units E of the VCL, in greenschist to lower amphibolite facies, were probably incorporated in the Variscan "supra-schlingen" nappe stack.

3) The "main schistosity" (S2) of the Ordovician metagranitoids ("orthogneisses") is most probably syn- to subsequent postmagmatic and is thus Ordov./Silur. in age. This conclusion has far-reaching implications for all pre-Mesozoic crystalline basement units in the Alps.

BORIANI, A., BURLINI, L. and SACCHI, R. (1990): The Cossato-Mergozzo-Brissago Line and the Pogallo Line (Southern Alps, Northern Italy) and their relationships with the late-Hercynian magmatic and metamorphic events. Tectonophysics, 182, 91–102.

CONEY, P.J. (1987): The regional tectonic setting and possible causes of Cenozoic extension in the North American Cordillera. Geol. Soc. Spec. Publ., 28, 177–186.

FLISCH, M. (1987): Teil 1: Geologische, petrographische und isotopengeologische Untersuchungen an Gesteinen des Silvretta-Kristallins. Teil 2: Die Hebungsgeschichte der oberostalpinen Silvretta-Decke seit der mittleren Kreide. Teil 3: K–Ar dating of Quaternary samples. Unpubl. Ph. D. Thesis, University of Bern, Switzerland.

HANDY, M.R. (1987): The structure, age and kinematics of the Pogallo fault zone; Southern Alps, northwestern Italy. Eclogae geol. Helv., 80/3, 593–632.

HOLLISTER, L.S. and CRAWFORD, M.L. (1986): Melt-enhanced deformation: a major tectonic process. Geology, 14, 558–561.

HUISMANS, R.S. (1994): Geology of the area of Passo St. Jorio: the Val Colla fault zone and Alpine shortening. Abstract at the 11th annual meeting of the Swiss Tectonic Studies Group, 25.–26. Februar 1994, Neuchâtel, Switzerland.

JONGMANS, W.J. (1960): Die Karbonflora der Schweiz. Beitr. geol. Karte Schweiz, N.F. 108.

LOESCHKE, J. and HEINISCH, H. (1993): Palaeozoic volcanism of the Eastern Alps and its palaeotectonic significance. In: J.F. VON RAUMER and F. NEUBAUER (eds): 1993, Pre-Mesozoic geology in the Alps, Springer-Verlag, Berlin, Heidelberg, 441–455.

MCDOWELL, F.W. (1970): Potassium-argon ages from the Ceneri zone, southern Swiss Alps, Contr. Mineral. Petrol., 28, 165–182.

NEUBAUER, F. and SASSI, F.P. (1993): The Austro-Alpine quartzphyllites and related Palaeozoic formations. In: J.F. VON RAUMER and F. NEUBAUER (eds): 1993, Pre-Mesozoic geology in the Alps, Springer-Verlag, Berlin, Heidelberg, 423-439.

PIDGEON, R.T., KÖPPEL, V. and GRÜNENFELDER, M. (1970): U–Pb isotopic relationships in zircon suites from a para- and ortho-gneiss from the Ceneri zone, southern Switzerland. Contr. Mineral. Petr., 26, 1–11.

SCHUMACHER, M.E. (1994): Die Grenze zwischen Val Colla-Zone und Ceneri-Zone: ein Schlüssel im südalpinen Grundgebirge. Abstract at the 11th annual meeting of the Swiss Tectonic Studies Group, 25.–26. Februar 1994, Neuchâtel, Switzerland.

ZURBRIGGEN, R. (1994): The tectonometamorphic history of schlingen in the Strona-Ceneri zone, a comparison to other schlingen areas, and the consequences. Abstract at the 11th annual meeting of the Swiss Tectonic Studies Group, 25.–26. Februar 1994, Neuchâtel, Switzerland.